

UNIVERSITY OF CALGARY

Analysis of Drilling Fluid Rheology & Pressure Drop Modelling to Improve
Drilling Efficiency

by

Kazi Mahmudur Rahman

A THESIS

SUBMITTED TO THE FACULTY OF GRADUATE STUDIES
IN PARTIAL FULFILMENT OF THE REQUIREMENTS FOR THE
DEGREE OF MASTER OF ENGINEERING

DEPARTMENT OF MECHANICAL AND MANUFACTURING ENGINEERING

CALGARY, ALBERTA

DECEMBER, 2018

© Kazi Mahmudur Rahman 2018

UNIVERSITY OF CALGARY
FACULTY OF GRADUATE STUDIES

The undersigned certify that they have read and recommend to the Faculty of Graduate Studies for acceptance, a Thesis entitled "Analysis of Drilling Fluid Rheology & Pressure Drop Modelling to Improve Drilling Efficiency " submitted by Kazi Mahmudur Rahman in partial fulfilment of the requirements of the degree of Master of Engineering.

*Supervisor, Dr. Robert Martinuzzi, Department of
Mechanical and Manufacturing Engineering*

*Dr. Les Jozef Sudak., Department of Mechanical and
Manufacturing Engineering*

*Dr. David Wood., Department of Mechanical and
Manufacturing Engineering*

*Dr. Hassan Hassanzadeh., Department of Chemical &
Petrochemical Engineering*

August 14, 2008

Date

Abstract

The major drilling problems such as fluid loss, wellbore strengthening, well control, carrying capacity, torque & drag, stuck pipe, etc. can result from the improper matching of drilling fluid properties. These problems occur due to variations in pressure, and temperature which has a great impact on the rheological properties. Drilling fluid properties can be modified for the successful drilling operation. Research continues the development of drilling fluid in shale inhibition, rheology modification, wellbore strengthening, high-temperature, high-pressure (HTHP) drilling fluids, etc. The main goal of this project is to develop a rheology-based pressure drop calculation incorporating the effects of temperature, pressure and gel strength of drilling fluid using experimental results for the better understanding of undesirable viscosity fluctuation and pressure losses. This study is based on the hypothesis that the rheology model for pressure loss prediction can be investigated to the desired level in an experimental laboratory facility, which can be applied to solve/reduce drilling problems in wells. This study presents a simplified procedure for selecting the rheological model which best fits the properties of a given hydraulic fluid to represent the shear-stress, shear-rate relationship for a given fluid. The project assumes that the model which gives the lowest absolute average percent error (EAAP) between the measured and calculated shear stresses is the best one for given drilling fluid. The results are of great importance for achieving the correct pressure drop and hydraulics calculations. It is found that the API rheological model provides, in general, the best prediction of rheological behaviour for the mud samples considered (EAAP= 5.84%). API hydraulics calculation gives a good approximation to measured pump pressure within 14% of measured field data.

Acknowledgements

I have had the good fortune to have enormous guidance from my supervisor, Dr. Robert Martinuzzi where his enormous support, ideas, motivation and helpful instructions gave me to make the successful completion of my thesis work. I am very happy to have the members of examining committee, Dr. Hassan Hassanzadeh, Dr. Les Jozef Sudak, and Dr. David Wood, in my thesis defence and would like to thank them for their valuable time and the discerning input to my thesis work. I would like to acknowledge the different financial supports of: (i) Dr. Robert Martinuzzi's various research grants, (ii) Teaching Assistantships. I also want to thank to my beloved family members for their encouragement and greatly appreciated and pleased to my dear wife, Musa. Shammi Akther for her enormous help and inspiration during the program to make it achievable.

Dedication

To the loving memory

of

My Parents

Table of Contents

Approval Page.....	ii
Abstract.....	iii
Acknowledgements.....	iv
Dedication.....	v
Table of Contents.....	vi
List of Tables.....	viii
List of Figures and Illustrations.....	ix
List of Symbols, Abbreviations and Nomenclature.....	x
CHAPTER 1: INTRODUCTION.....	1
1.1 Background.....	1
1.2 Problem statement.....	5
1.3 Research objectives.....	7
1.4 Thesis structure.....	7
CHAPTER 2: LITERATURE REVIEW.....	9
2.1 Drilling fluid rheology.....	9
2.2 Pressure and temperature effect in the rheology of drilling fluid.....	10
2.3 Rheology parameters.....	11
2.4.2 Concentration.....	13
2.4.3 Gel strength.....	13
2.4.4 Pressure loss.....	13
2.4.5 Friction reduction.....	13
2.4 Drilling Operation.....	14
2.5 Hydraulics.....	15
2.6 Frictional Pressure Loss.....	16
CHAPTER 3: METHODOLOGY.....	19
3.1 Fluid Preparation.....	21
3.2 Experiment Procedure.....	22
3.3 Rheological Model Selection.....	24
3.2.1 Correlations analysis.....	24
3.2.2 The absolute average percent of error (E_{AAP}) analysis.....	25
3.3.3 Determining parameters for the Rheology Models.....	25
3.3.3.1 Newtonian Model.....	25
3.3.3.2 Bingham Plastic Model.....	26
3.3.3.3 Power Law Model.....	26
3.3.3.4 API Model.....	26
3.3.3.5 Herschel-Bulkley Model.....	27
3.4 Hydraulics.....	28
CHAPTER 4: RESULTS AND DISCUSSION.....	
4.1 Fann Viscometer Reading.....	31

4.2 Error Analysis	32
4.3 Shear stress measured.....	32
4.4 Rheological Model Selection.....	33
4.4.1 Newtonian Model and Experiment data.....	33
4.4.1.1 Shear stress calculation	33
4.4.1.2 Correlations Analysis.....	34
4.4.1.3 The absolute average percent of error (E_{AAP}) analysis.....	35
4.4.2 Bingham Plastic Model and Experiment data.....	35
4.4.2.1 Shear stress calculation	35
4.4.2.2 Correlations Analysis.....	36
4.4.2.3 The absolute average percent of error (E_{AAP}) analysis.....	38
4.4.3 Power Law Model and Experiment data.....	38
4.4.3.1 Shear stress calculation	38
4.4.3.2 Correlations Analysis.....	38
4.4.3.3 The absolute average percent of error (E_{AAP}) analysis.....	40
4.4.4 API Model and Experiment data.....	40
4.4.4.1 Shear stress calculation	40
4.4.4.2 Correlations Analysis.....	40
4.4.4.3 The absolute average percent of error (E_{AAP}) analysis.....	42
4.4.5 Herschel-Bulkley Model and Experiment data.....	42
4.4.5.1 Shear stress calculation	42
4.4.5.2 Correlations Analysis.....	42
4.4.5.3 The absolute average percent of error (E_{AAP}) analysis.....	43
4.5 Summary of rheological model selection.....	44
4.6 Hydraulics Simulation.....	45
4.7 Data used to validate the approach.....	48
CHAPTER 5: CONCLUSIONS AND FUTURE WORK.....	50
5.1 Summary.....	50
5.2 Further considerations.....	50
REFERENCES.....	52

List of Tables

Table 3.1: Composition of the Fluid-1	21
Table 3.2: Composition of the Fluid-2.....	21
Table 4.1: Fann Viscometer Reading: Fluid-1.....	31
Table 4.2: Fann Viscometer Reading: Fluid-2... ..	31
Table 4.3: Shear stress measured in field units (lb/ft ²) for Fluid-1.....	33
Table 4.4: Shear stress measured in field units (lb/ft ²) for Fluid-2.....	33
Table 4.5: Comparison analysis between measured and calculated shear stresses.....	34
Table 4.6: Comparison analysis between measured and calculated shear stresses.....	36
Table 4.7: The measured and calculated shear stresses	38
Table 4.8 The measured and calculated shear stresses	40
Table 4.9 The measured and calculated shear stresses	42
Table 4.10: Summary of best regression equationfor Fluid-1	44
Table 4. 11: Summary of best regression equationfor Fluid-2	45
Table 4.12: Average % of reduction error difference between field and modeled SPP ...	48

List of Figures and Illustrations

Figure 1.1: Schematic comparison of the four rheological models	4
Figure 2.1: Rheograms at various temperatures and pressures (Davison et al. 1999). ...	11
Figure 2.2: Figure 2.2: Rheogram showing rheological types (Awele 2014).....	12
Figure 2.3: Diagram of the drilling fluid circulating system	18
F Figure 3.1: Flow chart for overall analysis and assessment of hydraulic performance in well applications	20
Figure 3.2: Schematic diagram of the Fann Model 35 viscometer	23
Figure 4.1: Residual plot for measured and calculated shear stress for Newtonian model.....	34
Figure 4.2: Plot for shear rate vs. shear stress of measured and modeled data using Newtonian model.	35
Figure 4.3: Residual plot for measured and calculated shear stress for Bingham Plastic model.....	37
Figure 4.4: Plot for shear rate vs. shear stress of measured and Modeled data	37
Figure 4.5: Residual plot for measured and calculated shear stress for Power Law	39
Figure 4.6: Plot for shear rate vs. shear stress of measured and calculated data	39
Figure 4.7: Residual plot for measured and calculated shear stress for API model.	41
Figure: 4.8: Plot for shear rate vs. shear stress of measured and calculated data.	41
Figure 4.9: Residual plot for measured and calculated shear stress for Herschel- Bulkley	42
Figure 4.10: Plot for shear rate vs. shear stress ...data for Herschel-Bulkley model.	43
Figure 4.11: Average % of reduction error difference between field SPP and modeled SPP	49

List of Symbols, Abbreviations and Nomenclature

List of Symbols

<u>Greek symbols</u>	<u>Definition</u>
γ	Shear rate, s-1
ρ	Mud weight
τ	Shear stress, lb/100ft ²
τ_0	Yield point, lb/100ft ²
Θ_3	Dial reading at 3rpm
μ_p	Plastic viscosity
τ_y	yield point
τ_0	yield stress
μ	Viscosity

List of Abbreviations

<u>Abbreviation</u>	<u>Definition</u>
NP	Nanoparticles
API	American Petroleum Institute
PV	Plastic viscosity
OBM	Oil Based Mud
SBM	Synthetic mud
Δp_a	Pressure loss in annulus, psi
Δp_b	Pressure loss in bit, psi
Δp_{ds}	Pressure loss in drill string, psi
Δp_p	Pump pressure, psi
HHP	High-pressure
ECD	Equivalent circulating density
EAAP	Absolute average percent error
YP/PV	Ratio of yield point over plastic viscosity
EMW	Equivalent mud weight
MWD	Measurement-while-drilling
YP	Yield points
K	Consistency index
n	Fluid behavior index
Δp	Pump pressure
PVT	Pressure/volume/temperature
Q	Flow rate of the drilling fluid, gpm
N	Rotational velocity, rpm
cp	Bingham Yield Point, lb/100ft ²

CHAPTER 1: INTRODUCTION

1.1 Background

Drilling operations are required to achieve a well safely within shortest possible time and lowest possible operational cost, including the necessary additional sampling and evaluation constraints of the particular application to reduce drilling problems (Proehl and Sabins 2006, Taugbol et al. 2005). Drilling problems include fluid loss, wellbore stability, well control, poor carrying capacity, poor torque performance increased drag and stuck pipe. These can result from poorly defined drilling fluid and often result in high drilling cost. Around one fifth (15 to 18%) of the total cost (about \$1 million) of well petroleum drilling are related to the drilling fluid (Khodja et al. 2010a). Problems occur due to variations in pressure, temperature, which affect the fluid rheological properties (viscosity) during drilling operations. The fluids should generally meet some important specified requirements: i) fluid rheological characteristics that are easily controlled, ii) not too expensive and iii) environmentally friendly (Khodja et al. 2010b). Drilling fluids should reduce the cleaning cost and time, maximize recycling to reduce the environmental footprint. Consequently, environmentally compatible successful completion of drilling operation depends on the properties of the drilling fluid to a great extent. Therefore, the choice of the right fluid (right properties) is very important in fluid design and drilling waste management during drilling operation which influences the total well operations costs and improved drilling efficiency.

Rheological properties provide assistance in characterizing fluid flow. When determining the flow characteristics, the rheology is important for predicting friction coefficients and frictional pressure losses. Rheological parameters such as viscosity, consistency index, and yield stress control the fluid system under consideration, together with volumetric parameters such as density (Demirdal et al 2009). All these parameters are subject to change under extreme conditions such

as high pressure-high temperature or low pressure-low temperature conditions (Friedheim et al 2012). The pressure and temperature have direct effects on drilling fluid rheology through the shear stress and shear rate of the fluid (Garvin et al 1970, DE Wolfe et al 1983, Minton & Bern 1988, American Petroleum Institute 1995). Drilling fluids used in drilling operations have rheological properties and density which are more sensitive to pressure and temperature conditions (Hemphill 1996, Growcock 1994, Growcock & Frederick 1994). For this reason, it is important to determine the response of the rheological model to wellbore conditions and to fully understand the fluid performance under downhole conditions.

As the well goes deeper, it becomes increasingly important to predict and control the rheology of drilling fluids and hydraulics of the well. Rheological models are adopted for prediction and calculation of the shear stress and frictional pressure losses. The most used rheological models for the past half-century are Newtonian, Bingham and Power-law models. With the development of drilling fluid technology and drilling hydraulics theory, the limitations of the Bingham and Power Law models have been identified by researchers. The main disadvantage is the two models are not able to describe the rheological properties of drilling fluid under high shear rates. The Herschel-Bulkley model is a newer rheological model that accurately describes the rheological properties of drilling fluid under a wider range of shear rates (Power, 2003). It is characterized by a nonlinearity relationship between shear stress and shear rate and comprises the yield point (Power & Zamora, 2003). API (American Petroleum Institute) recommended predicting fluid behaviour with a two-part power law model. One part predicts the fluid behaviour at low shear rates, and another part modelled the high shear properties (Rehm et al, 2012). So, this model endorses using the modified power-law model to calculate pressure losses in pipes and annuli. Generally, the drilling fluid apparent viscosity decreases with increasing shear rate. The

power law matches shear rates from the viscometer with shear rates experienced inside the drill pipe and annulus. Inside the drill pipe, 600 RPM and 300 RPM viscometer readings are used for rheology and pressure loss calculations (API 1995).

This study presents the comparison of several major rheological models to select the best one for representing the relationship between shear stress and a shear rate of fluid. The models considered are the Newtonian, Bingham, Power-law, API Power law and Herschel-Bulkley models. The shear stress versus shear rate data is used to determine which rheological model best fits the behaviour of the fluid system.

Drilling fluids are classified into two major groups: Newtonian fluids where viscosity, μ , is independent of shear rate and the non-Newtonian fluids where viscosity is a function of shear rate, $\mu = \mu(\dot{\gamma})$. Viscosity measures the resistance to flow. Excessive viscosity is undesirable because of the pressures that can be generated by a higher viscosity in the borehole when pumping horizontally. For each fluid, there is a constitutive relation between the shear rate ($\dot{\gamma}$) and shear stress (τ). To model the shear stress-shear rate behaviour of fluids, mathematical relations known as rheological models are used.

A general graphical representation of the four discussed rheological models is presented in Figure 1.1. The best fitted rheological model will be more tuned with variation of temperature/pressure, and flow rate. The good model will predict the performance of fluid behaviour and thus allow reducing the pump requirements and reduce drilling unstableness/problems (i.e.; fluid loss, carrying capacity, formation damage, etc. among others.).

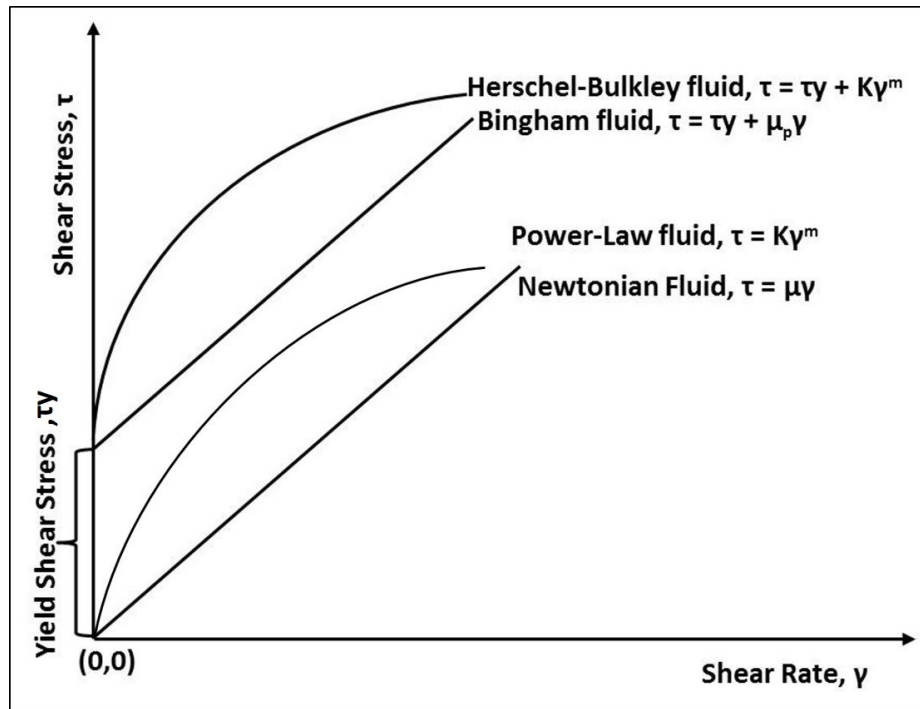


Figure 1.1: Schematic comparison of the four rheological models

Fluid rheological properties change with additives and can be matched to fulfill the specific requirements for the hydrodynamic properties and interaction potential with the formation (Amanullah et al 2011, Abdo & Haneef 2010, Srivista 2010). Increases in viscosity reduce the penetration rate, increase frictional pressure loss in the drill pipe and annulus, and increase the horsepower requirement of the pump (Cranford et al 1999, Mohammed & Mohammed 2009). Thixotropic shear thinning fluids with a yield stress occurs with the apparent viscosity decreases with increasing shear rate, are often used to avoid high-pressure drop when the mud is circulated upward the annular, and the presence of a yield stress avoids the sedimentation of solids cuttings and barite when the circulation is stopped for a certain amount of time (Herzhaft et al 2006).

The drilling process can be improved by controlling the drilling fluid properties using a macro/micro size chemical particles/additive (Zakaria et al 2012, Nwaoji et al 2013). These

particles are smaller than microparticles, have a high surface to volume ratio and may provide superior fluid properties at low concentration of the additives (Amanullah & Al-Abdullahtif 2010). Additives like nanoparticles, which have smaller size, surface area and higher surface energy, can control the rheology of fluid properties to a larger extent when compared to micron-sized particles (El-Diasty et al 2013, Amanullah et al 2011). Due to the strong particle-particle interaction, many additives can act as viscosifiers. For a drilling fluid, the desired rheological effect from an additive varies widely depending on the ultimate goal of hole cleaning (high low-shear rate), the reduction of equivalent circulating densities (ECD) with lower plastic viscosities (PV) and yield points (YP), or the minimization of the effect that temperature has on viscosity (Demirdal et al 2009). The rheological effects can be measured through the physical fluid properties like density, viscosity, gel strength, etc. characterize the drilling fluid. Among different drilling fluids, nanoparticles-based drilling fluids result in higher performance compared to non-nano-based drilling fluid (Zakaria et al 2012, Nwaoji et al 2013). Nanoparticles-based drilling fluid application is an enhanced drilling fluid technology for the successful drilling operation (El-Diasty et al 2013, Amanullah et al 2011). Research continues the development of nanoparticles-based fluid in shale inhibition, rheology modification, wellbore strengthening, high-temperature, high-pressure (HTHP) drilling fluids, etc. (Zakaria et al 2012, Nwaoji et al 2013, Hoelscher et al 2013, Friedheim et al 2012). Variations in pressure, and temperature, which affect the fluid rheology and phase volume ratio in drilling fluids are important considerations for drilling operational problems (Gusler et al 2007, Lee et al 2012).

1.2 Problem statement

Rheological properties are important for assessing the drilling fluid behaviour in solving

problems of hole cleaning, hole erosion, suspension of cuttings, drilling fluid treatment, and hydraulics calculations. Hydraulics calculations with the best-fitted rheology models are the focus of this project. The viscosity of the drilling fluid must be known because it determines the hydraulics in the well. The rheological properties vary depending on the type of fluid. The rheological model used for the evaluation of the fluid parameters is thus important. The rheology of the most common drilling fluids today, is complex because they usually exhibit non-Newtonian behaviour. This study examines five major rheological models (Newtonian, Bingham, Power law, API Power Law, Herschel-Bulkley) to identify alternatives for selecting the model that represents most accurately the shear stress / shear-rate relationship for a given fluid. This approach assumes that the model that gives the lowest absolute average percent error (E_{AAP}) between the measured and calculated shear stresses is the best one for a given non-Newtonian fluid. In the present industry practice, calculated and actual pump pressures, for example, pressure drop, Δp calculations using API with a synthetic based mud (SBM) can be off by as much as 35% (API, 1995). The possible reasons could be that friction pressure losses calculations are not well represented by the rheological model (Zamora & Power, 2002). As a result, drill string pressure losses are underestimated (Thivolle, 2004).

Many experimental studies deal with the flow of fluids through pipes and annuli for friction pressure loss calculations. Most of these studies have concentrated on rheological models, pipe roughness, and geometrical parameters. However, the selection of the best rheological model to obtain correct results for pressure drop and hydraulics is not considered in the API models. This study of five rheological models is expected to serve as a guide for selecting a rheological model for the drilling fluid, for hydraulics calculation. This study could also be used in an educational engineering and for training purposes; it would help inform and educate the industry about

rheology in drilling fluid and hydraulics calculation considering different rheological models.

1.3 Research Objectives

In the thesis, the overall goal was to improve drilling efficiency and reduce drilling operational cost. Therefore, this study specifically focuses on:

- a) Determining fluid rheological behaviour, based on characteristics from the laboratory experiments;
- b) Investigating the best fitted rheology model for a drilling fluid;
- c) Calculating the hydraulics using best fitted rheology modelling for the fluid in terms of pressure drop calculation;
- d) Assessing the rheology/ pressure drop model incorporating the effects of drilling fluid with the help of experimental results for better understanding of undesirable viscosity fluctuation and pressure losses during drilling operation;
- e) Predicting bit wear and fluid degradation due to variation on total pressure losses;
- f) Increasing drilling efficiency via hydraulics optimization on drilling bit related to rheological properties.

1.4 Thesis Structure

The first part of this study presents a simplified and accurate procedure for selecting the rheological model which best fits the rheological properties of a given fluid. The outcomes are methods to select the best rheological model and to estimate frictional pressure loss from expansion and contraction of the fluid flowing through pipe and annuli. These methods are of great importance in achieving correct results for pressure drop and hydraulics calculations. Experimental

results were analyzed for Newtonian, Bingham, Power law, API Power Law, and Herschel-Bulkley models for conditions where, API hydraulics calculation gives a good approximation of measured pump pressure.

This thesis consists of five chapters. Chapter one describes the background of the research, problem statement, and objectives of the research. Chapter two provides the literature review with a brief description of different rheology models. Chapter three illustrates the methodology of the study. Chapter four provides the results of this research and includes a brief discussion on the findings. Chapter five summarizes the key findings of the research along with the scientific contribution of the research, and the future works.

CHAPTER 2: LITERATURE REVIEW

2.1 Drilling Fluid Rheology

In drilling operations, rheological properties indicate the character of deformation and flow of drilling fluid. The drilling fluid behavior can be evaluated in solving problems of hole cleaning, mud treatment, and hydraulics calculations. The character is usually described by the parameters: Apparent Viscosity (μ_a), Plastic Viscosity (μ_p) and Yield Point (τ_y). Viscosity is a property that indicates the resistance of drilling fluid to flow, defined as the ratio of shear stress to shear rate. Apparent viscosity is the viscosity measured at a given shear rate at a fixed temperature. Most drilling fluids exhibit plastic behavior, which can be described through τ_y .

Plastic fluids require a certain value of shear stress for initiating flow, which is characterized by the yield point. Plastic viscosity is the slope of the shear stress/shear rate curve above the yield point. It represents the viscosity of a mud based on the Bingham model when extrapolated to an infinite shear rate. The ratio of the yield point to the plastic viscosity (YP/PV ratio) is a measure of flattening of the flow profile. Higher YP/PV ratios provide better cuttings transport in laminar flow. Most drilling fluid muds are non-Newtonian fluids, and are shear thinning with viscosity decreasing as shear rate increases (Thivolle, 2004). Herzhaft et al. 2002, showed that plastic viscosity is the parameter most affected by temperature changes. In Deepwater wells, the cooling effect of the riser will result in higher plastic viscosity in the drilling fluid. Additionally, the length of the riser enhances the cooling effect during circulation and during trips, creating major changes in rheology if oil-based or synthetic mud is used. Changes in mud viscosity may also lead to problems with surge and swab, transmission of measurement-while-drilling (MWD) pulses, increased equivalent circulating density and variations in hole-cleaning efficiency.

Zamora and Power, 2002; detailed in their paper a new unified rheological model. The

rheological parameters for this model are the plastic viscosity (μ_p), yield point (τ_y) and yield stress (τ_0). A fourth parameter, τ_y , is a useful tool to help characterize fluids rheologically, although it is not necessary for solving the model. However, API RP 13D elements are still valid and in use, but some need to be updated. Mud rheology needs adjustment for downhole conditions, especially in ultradeep water wells drilled with oil or synthetic mud. Power and Zamora, 2003; showed that the ratio τ_0/τ_y is a useful parameter to characterize fluids rheologically. The acceptable range of τ_0/τ_y values is 0 to 1 for rheological models used in drilling.

2.2 Pressure and Temperature Effect in the Rheology of Drilling Fluid

Physically: An increase in temperature decreases the viscosity of the fluid and an increase in pressure increases the density, and viscosity of the fluid.

Chemically: Temperature has effects on alkalinity of the fluid which causes the thinner properties of the fluid and has effects on flocculation/deflocculating/aggregation process in the fluid.

Politte 1985; concluded from his analysis of rheological data for emulsion that drilling fluid yield point is not a strong function of pressure and becomes progressively less so as temperature increases. The effects of temperature on the yield point, however, are difficult to predict as they require chemical particle effects. Davison et al. 1999; concluded from their study of rheological data obtained from a viscosity meter that the effect of low temperature on both oil-based mud (OBM) and synthetic mud (SBM) viscosity is pronounced. On the other hand, when pressure was increased at various temperatures, viscosity of both oil based and SBMs increased, especially at higher shear rates (Figure 2.1). The pressure effects do not appear to be dependent on the temperature (Figure 2.1).

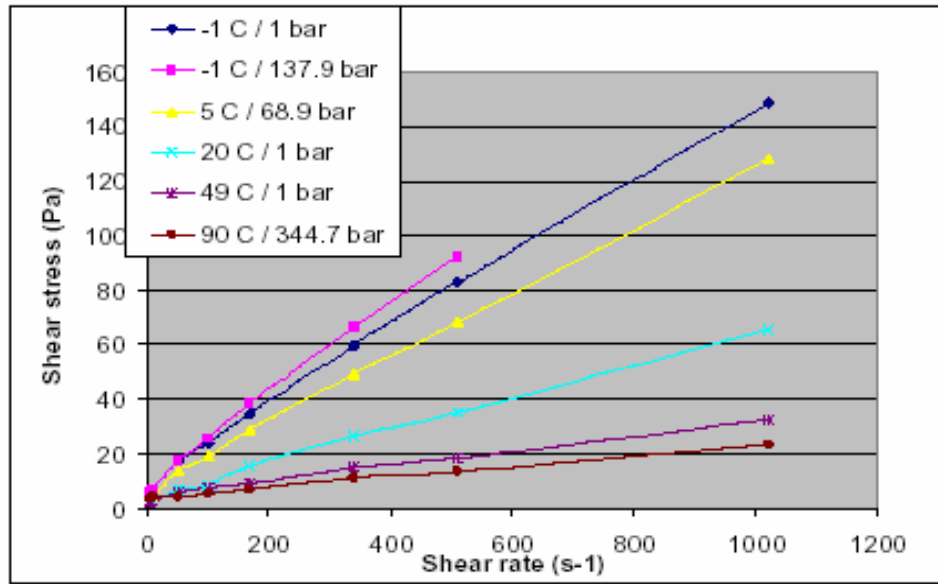


Figure 2.1: Rheograms at various temperatures and pressures for unweighted oil-based mud, 80:20 oil/water ratio (Davison et al. 1999).

Figure 2.1 also shows some results where; the prediction of hydrostatic pressure requires pressure/volume/temperature (PVT) data for the mud in addition to an accurate simulation of the downhole temperature profile. The compressibility of a drilling fluid depends on its base fluid. Zamora and Power, 2002; evaluated the inability of API equations from RP 13D to match field data in critical drilling, because these equations must incorporate the effects of temperature and pressure on density and rheological properties.

2.3 Rheological Parameters

The rheological characteristics of drilling fluids with yield point, gel strength and the rheological properties are tested throughout the drilling operations to characterize the behaviour of drilling fluids. These properties are often dependent on the relevant shear rates and timescales as well as sample size and viscosity in the laboratory experiment using the rheometer for measuring. Rheological properties most often defined by the rheogram and rheological parameters.

The parameters refer to the Bingham plastic fluid parameters: PV (Plastic viscosity) and YP (yield point), the power-law fluid model parameters: power law index (n) and consistency (K). There are four basic flow types: Newtonian fluid, Plastic fluid, Pseudoplastic fluid and Dilatant fluid, shown in the below figure 2.2.

In this figure 2.2, the four basic rheological fluid types are shown: 1) plastic fluids, which are characterized by a yield point ($YP = \tau_y$) and a constant plastic viscosity (PV) relating the shear stress, τ , to the shear rate, $\dot{\gamma}$; 2) pseudoplastic fluids for which $\tau_y = 0$; 3) Newtonian fluids, for which PV is constant and $\tau_y = 0$; 4) Dilatant fluids or shear thickening fluids.

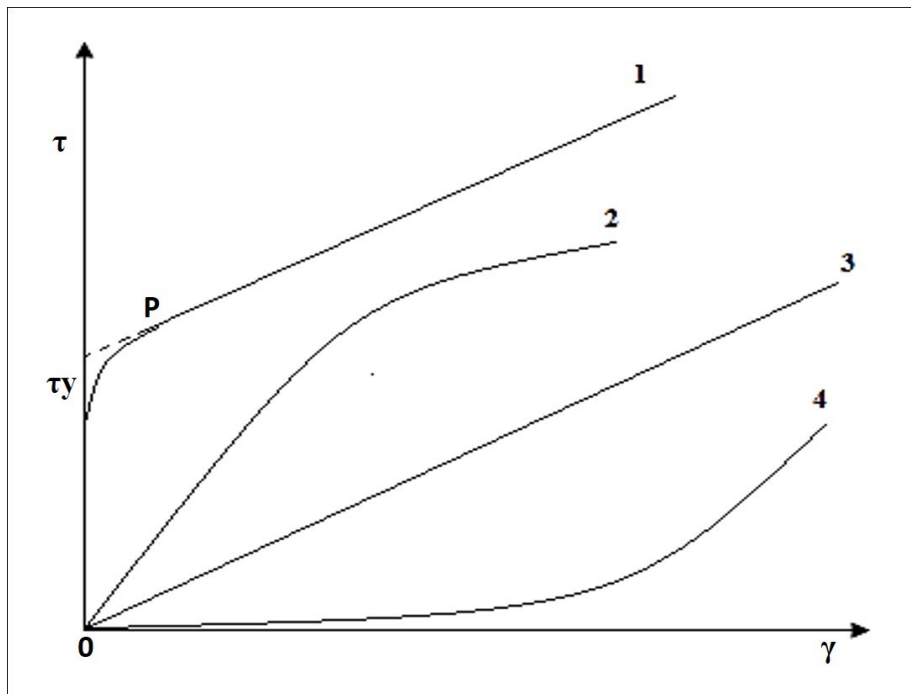


Figure 2.2: Rheogram showing rheological types (Awele 2014)

1-Plastic fluid; 2- Pseudoplastic fluid; 3- Newtonian fluid; 4-Dilatant fluid; τ - Shear stress, lb/100ft² or Pa; $\dot{\gamma}$ - Shear rate, s⁻¹; τ_y -YP = Yield point, lb/100ft² or Pa; PV-Plastic viscosity, cp or mPa·s

In the drilling process, good shear thinning behavior to drilling fluid is required, which means in low shear rate, the mud has high internal force, while in high shear rate, the mud has low internal force. It also means that the apparent viscosity (AV) decreases with the increasing shear rate. Normally the shear thinning behavior is characterized by the ratio of yield point over plastic viscosity (YP/PV) ratio. The higher YP/PV the better the shear thinning behavior.

From the shear stress and shear rate diagram (figure 2.2), it will be noticed that PV and YP are important properties of the drilling fluid. If additions of nanoparticles (NP's) change PV or YP, there will be an effect on the during drilling use. If NPs addition increase PV: 1) Equivalent circulating density will be increased and 2) Pump Pressure will be increased. A decrease will affect on carrying capacity of drilled cuttings. Again, if addition of NPs increases YP, similar affect can happen but moderate increase YP is good in terms of carrying capacity of drilled cuttings. YP is the stress required to initial flow of fluid after circulation is stopped. Due to flow of fluid friction coefficient need to measure as it can predict the wear rate of mechanical parts of the known fluid system and simulates the rotational velocity of drilled pipe.

2.3.1 Concentration

Fluids additives change/addition has influence of concentration based on viscosity and density.

2.3.2 Gel strength

Characterize the gel limit by relating the yield stress as a function of additive concentration.

2.3.3 Pressure loss

Pressure losses affect the Fanning friction factor, which is a function of the Reynolds number and the roughness of the pipe wall.

2.3.4 Friction reduction

For reducing the friction loss, shear thinning is a result from a reduction in structural viscosity and the mechanism of friction reduction is a result from the elastic properties of the long-chain polymers, which enable them to store the kinetic energy of turbulent flow.

Electrochemically: An increase in temperature increases the ionic activity of the electrolyte and solubility of salts that may be present in the mud. The magnitude and direction of these changes and their effects on rheology of the mud varies with the electrochemistry of the particular mud.

Thixotropic condition: It is a function of shear stress, shear rate, torque, and time. The viscosity of a thixotropic fluid depends on time of shearing, as well as rate of shear, because the structural component changes with time according to the past shear trend of the fluid.

2.4 Drilling Operation

The standard operation is that the drilling fluid supplied by a pump from the surface area through a drilling string to the drill bit in the wellbore (figure 2.3). The operation consists in adjusting fluid pressure drop across the drill bit and in the annulus. The drilling fluid hydraulics are to be optimized for the given drilling mud condition. In the drilling operation process, it is expected to lose a proportion of power due to friction. The drilling fluids are easy to use due to their stability at high temperatures and having high tolerance to solids to make them ideal for high pressure and high temperature (HPHT) wells (Maghrabi et al. 2011, Sushant et al. 2011). Its lubricity reduces the torque and drag and helps minimizing the potential for differential sticking where the rheology of the fluid flow characteristics is important (Mohamed et al. 2005). The functions of drilling fluids are to: (i) carry cuttings and clean the wellbore; (ii) cool and lubricate the bit and pipe in the wellbore; (iii) made good filtration and maintain the stability of the uncased formation; (iv) to stabilize and offset the formation pressure; and (v) balance the hydraulic horsepower.

During drilling operation there are several contaminants including solids and additives affecting the fluid hydraulics and in mud properties coming from the formation fractures and makes the fluid operation unstable. This contamination problem affects in fluid rheological properties and fluid hydraulics directly. Two concerns in determining the rheological properties of emulsions (Lee et al. 2012), are: (i) their effects on emulsion stability; and (ii) the effects of deterioration of the emulsion on its rheological properties. The flow properties of fluids are influenced by the principle factors which are: dispersed phase, continuous phase and emulsifying agent. The rheological properties of fluids affect the change in one or more of these factors. The factors that related to the dispersed phase are: (i) concentration (i.e. phase volume ratio); (ii) viscosity; and (iii) size of the particles (Gusler et al. 2007, Darley and Gary 1988).

The flow of fluid in porous media is also affected by the rheological properties. These control the loss of drilling fluid to high-permeability formations and within natural or induced fractures in the rock (Tehrani 2007). High concentrations of solids reduce drilling rates because they increase fluid density and viscosity (Kassab et al. 2011). Therefore, the drill bit hydraulic characteristics are the major parameter influencing drilling performances.

2.5 Hydraulics

Hydraulic power is one of the most important hydraulic parameters having a major impact on the rate of penetration. In drilling operation, the conventional calculations of downhole pressure, which assume constant drilling fluid properties, are both practical and accurate enough for drilling well applications. Downhole static pressures are easy to calculate from mud weight measured at the surface, while additional pressures caused by circulation can be calculated using established relationships between pump rate and drilling fluid rheological properties (Merlo et al. 1995). Errors that result from ignoring variations in mud properties are small in relatively shallow

wells. In these settings, mud engineers can concentrate on formulating drilling fluid properties for maximum rates of penetration and optimal hole conditions. Formations can commonly withstand moderate overpressure before being fractured, which permits mud engineers to add a safety margin when weighting the mud (Merlo et al. 1995). In contrast, in high pressure and high temperature (HPHT), extended reach, and deep-water wells, mud properties vary significantly with downhole pressure and temperature, affecting the accuracy of both surface measurements and downhole estimations of mud weight and viscosity. In these wells these variations can be significant because of the limited safety margins available (Merlo et al. 1995).

The ability to predict the effects of rheological changes are critical to the successful drilling of HPHT, extended reach, and deep-water wells. Small but serious errors in computing the drilling fluid pressure at the reservoir may result from ignoring uncertainties in either temperature or fluid properties. Simulation of downhole temperature profiles at all phases of the drilling operation is therefore the key to understanding the behavior of drilling fluids (Zamora et al. 2005). Equivalent circulating density (ECD) is often much higher than equivalent mud weight (EMW) in HPHT, extended reach, and deep-water wells due to the small annular clearances between the drill pipe and hole wall. ECD is computed from the dimensions of the annulus and, fluid viscosity, and pump rate. The calculation becomes increasingly complicated when changes of viscosity with temperature are considered (Merlo et al. 1995).

2.6 Frictional Pressure Loss

Frictional pressure loss is a function of several factors such as rheology of the drilling fluid (Newtonian or non-Newtonian), flow regime (laminar, turbulent, or intermediate flow), flow rate, drill string configuration and wellbore geometry.

During circulations of the drilling fluid through the well fluid circulating system (Figure 2.3), friction between the drilling fluid and the wall of the drill pipe and annulus cause pressure loss.

The pump pressure, ΔP_p , is affected by:

1. Frictional pressure losses (ΔP_s) in the surface equipment such as Kelly, swivel, and standpipe.
2. Frictional pressure losses (ΔP_{ds}) inside the drill string (drill pipe, ΔP_{dp} and drill collar, ΔP_{dc}).
3. Frictional pressure losses across the bit, ΔP_b .
4. Frictional pressure losses in the annulus around the drill string, ΔP_a .

Mathematically the total pump pressure normally calculates by summation of all the above frictional pressure losses ($\Delta P_p = \Delta P_s + \Delta P_{ds} + \Delta P_b + \Delta P_a$). It is also known as stand pipe pressure (SPP): Error in ΔP_p is a combination of errors in the four elements. In general, frictional pressure losses across the bit, ΔP_b , and the surface pipe system can be evaluated accurately. Error in ΔP_p consists primarily of errors from friction pressure losses in the drill string and annulus. The drill string pressure losses represent the largest component of error in the pump pressure.

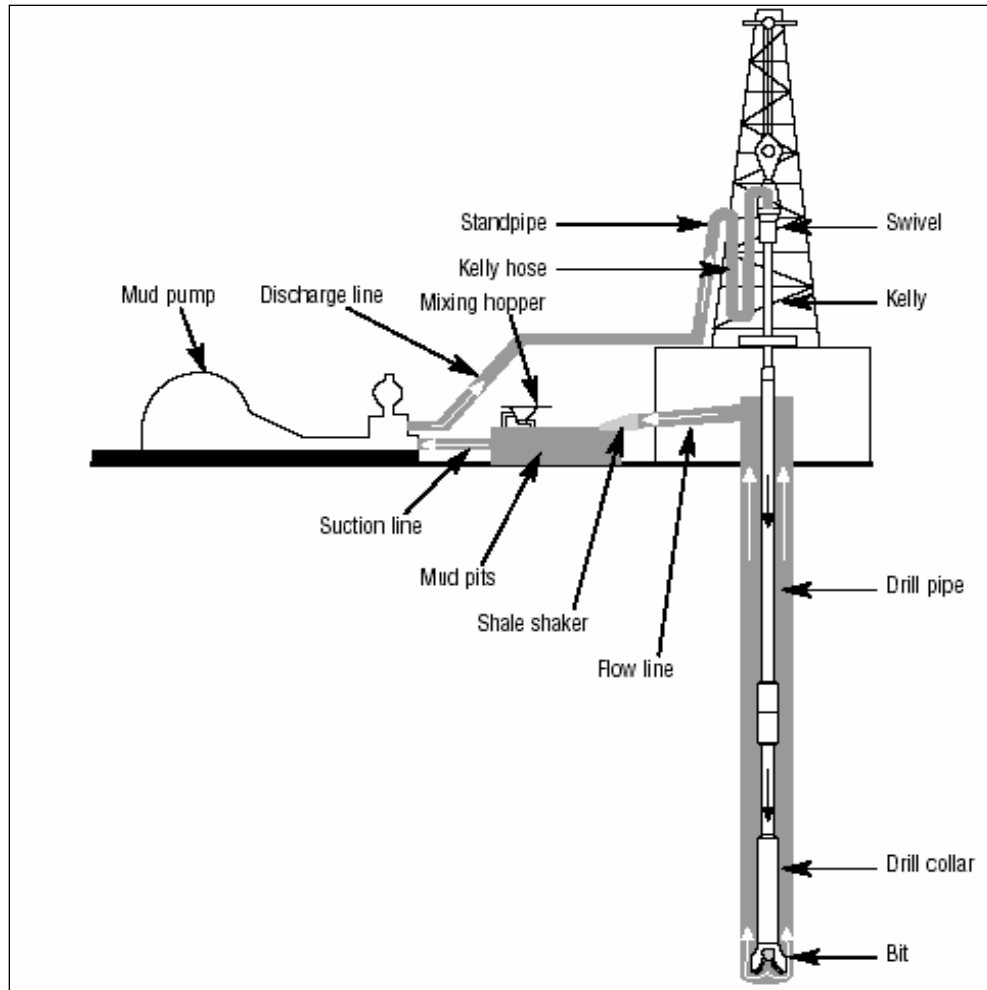


Figure 2.3: Diagram of the drilling fluid circulating system.

The diagram of the drilling fluid circulating system (figure 2.3) shows that the fluid flows throughout the drill pipe, drill collar, drill bit. Thereby the pressure drop occurs through each section in the wellbore and surface to be reduced to increase the drilling efficiency.

CHAPTER 3: METHODOLOGY

In this chapter, the methodology of determining the fluid viscosity and selection of rheological model is described. The procedure for predicting the hydraulic pressure loss, based on the rheological properties and models, is summarized. Considerations for the error analysis are given. Figure 3.1 provides a flow chart for the overall procedure, starting with the determination of rheological properties, simulation of hydraulic pressure loss and comparison to experimental or field data for assessment leading to recommendation.

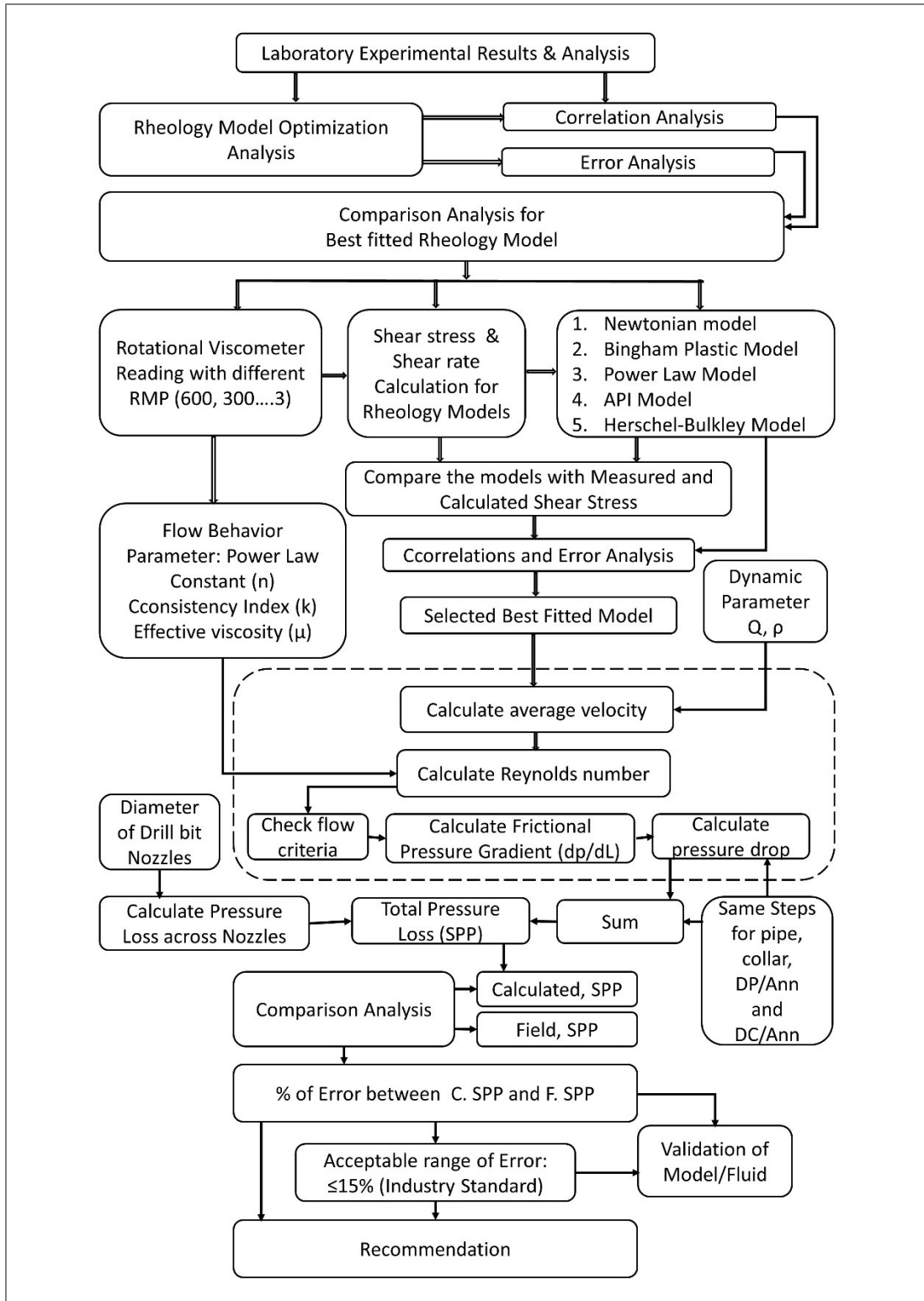


Figure 3.1: Flow chart for overall analysis and assessment of hydraulic performance in well applications

3.1 Fluid Preparation

Fluid samples, containing water and additives includes: clay, salts, caustic soda, polymer, starch, (See Table 3.1) were prepared by adding together and mixed well. This fluid sample was named “Fluid-1”. The composition ratio was maintained constant for all subsequent fluid samples used in the lab work. The rheological properties of these fluids were measured and recorded. All rheological properties were measured at ambient conditions (at 20⁰C).

Table 3.1: Composition of the Fluid-1

Chemicals for Fluid-1	Concentration unit		Metric unit	1000 ml	
NaCl	26	lb/bbl	9.12	kg/m ³	9.12g
Amine	6	lb/bbl	2.11	kg/m ³	2.11g
XC polymer	1.5		0.53	kg/m ³	0.53g
Clarified Starch	8	lb/bbl	2.81	kg/m ³	2.81g
CaCO ₃	35	lb/bbl	12.28	kg/m ³	12.28g

Table-3.2 described for the composition analysis of another water-based mud as Fluid-2 and done the same comparison analysis.

Table 3.2: Composition of the Fluid-2

Chemicals for Fluid-2	Concentration unit		Metric unit	1000 ml	
Xanthan gum	3	lb/bbl	1.15	kg/m ³	1.15g
PAC LV	2.5		2.53	kg/m ³	2.53g
Starch	10	lb/bbl	5.20	kg/m ³	5.20g
NaOH 5M	5	lb/bbl	2.28	kg/m ³	2.28g

The desired concentration of fluid solutions was prepared by dissolving of the polymer in water by stirring of the mixture with the magnetic stirrer at 1000 rpm until the polymer is fully dissolved. The fluids solution in each concentration was incubated at temperature points ranging

from room temperature (20⁰C) for about an hour at each point. Once the thermometer indicated that the solution temperature is constant, the dial readings were performed by viscometer and rheological parameters were calculated. The concentration (m/v) of each fluid solution, which provided the highest ratio of yield point over plastic viscosity (YP/PV ratio), was considered as the optimum concentration and was selected for the next analysis.

3.2 Experiment Procedure

To measure the rheological parameters of the drilling fluid a FANN Model 35 Viscometer was used. The FANN Model 35 viscometer is a rotational instrument powered by an electric motor. The test fluid is contained in the annular space (shear gap) between two concentric cylinders. The outer cylinder or rotor sleeve is driven at a constant rotational velocity. The rotation of the rotor sleeve in the fluid sample produces a torque on the inner cylinder or bob. A torsion spring restrains the movement of the bob, and a dial attached to the bob indicates displacement of the bob.

A schematic diagram of the direct indicating viscometer is shown in Figure 3.2. The deflection in degrees of the bob is read from the graduated scale on the dial. The viscosity of the samples was measured at the rotational velocity of 3, 6, 100, 200, 300 and 600 rpm. Shear rate is proportional to rotational velocity. According to the dial reading at different rotational velocity, the rheological parameters (PV and YP) are calculated according to:

$$\mu_p = \theta_{600} - \theta_{300} \dots\dots\dots (3.7)$$

$$\tau_y = \theta_{300} - \mu_p \dots\dots\dots (3.8)$$

Where: γ -shear rate, s^{-1} ; N-rotational velocity, rpm; θ_{600} -dial reading of 600rpm, θ_{300} -dial reading of 300rpm, μ_p -Plastic Viscosity, cp; τ_y -Bingham Yield Point, lb/100ft².

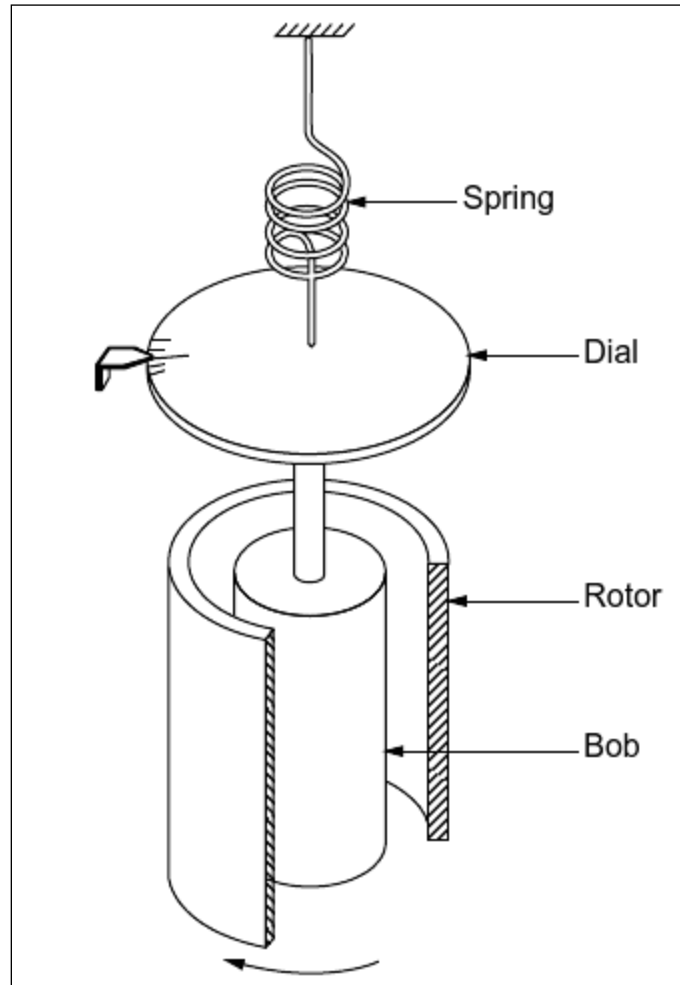


Figure 3.2: Schematic diagram of the Fann Model 35 viscometer

Three trials were done to determine the rheological parameters for fluid sample. Two fluid samples were tested. The results are reported as the ensemble average:

$$\bar{S} = \frac{1}{N} \sum_{n=1}^N S_n$$

Where S is the property and $N = 6$ is the total number of samples. The variance of the experiments:

$$\delta_s = \sqrt{\bar{S}^2} = \frac{1}{N-1} \sum_{n=1}^{N-1} (S_n - \bar{S})^2$$

is reported as an estimate of the measurement uncertainty.

3.3 Rheological Model Selection

This study presents a comparison of several major rheological models to select the best one which precisely represents the relationship of shear stress and shear rate of the fluid solutions. These models are the Newtonian, Bingham, Power-law, API dual Power-law and Herschel-Bulkley. The shear stress versus shear rate data is plotted for determining which rheological model best fit the behavior of the fluid system. Comparison analysis has done in two ways; (i) Correlations Analysis, and (ii) The absolute average percent of error (E_{AAP}) analysis.

3.3.1 Correlations Analysis:

Correlation analysis involves identifying the relationship between a dependent variable and one or more independent variables. A model of the relationship is assumed and estimates of the parameter values are used to develop an estimated regression equation. The regression analysis (value of R^2 -value) between the measured and calculated shear to determine the correlations of the best fitted model. The model that gives the highest R^2 -squared value is the best one for a given drilling fluid.

The regression analysis was based on residual plots. A residual is the difference between the measured value and the predicted value of a regression model. It is important to understand residuals because they show how accurate a mathematical function, represents a set of data. In a graph that shows the residuals on the vertical axis and the independent variable on the horizontal

axis. If the points in a residual plot are randomly dispersed around the horizontal axis, a linear regression model is appropriate for the data; otherwise, a non-linear model is more appropriate.

3.3.2 The absolute average percent of error (E_{AAP}) analysis

The absolute average percent error (E_{AAP}) between the measured and calculated shear stresses is the criterion for selecting the model. It is the analysis to determine the best fitted model that is applied in pressure loss calculations. The model that gives the lowest EAAP is the best one for a given drilling fluid.

The lowest E_{AAP} between the measured and calculated (predicted using the model relationship) shear stress is the criterion for selecting the model of a given drilling fluid:

$$E_{AAP} = [(1/N) \sum |(\tau_{measured} - \tau_{calculated}) / \tau_{measured}|] \times 100 \dots \dots \dots (3.9)$$

3.3.3 Determining parameters for the Rheology Models

3.3.3.1 Newtonian Model

Newtonian fluid has linear relationship between shear stress (τ) and shear rate (γ) according to:

$$\tau = \mu\gamma \dots \dots \dots (3.10)$$

Where: τ = shear stress, lb/100ft² or Pa,

μ = viscosity, cp or mPa·s,

γ = shear rate, s⁻¹

Here, the shear stresses can be estimated as function of viscosity and calculated by the following equations:

$$\mu = \Theta_{300} \dots \dots \dots (3.11)$$

$$\text{Calculated Shear Stress, } \tau = \frac{\mu}{478.8} \gamma \dots \dots \dots (3.12)$$

Where: Θ_{300} = dial reading of viscometer at 300 rpm; and 1 lb/100ft² = 478.8cp.

3.3.3.2 Bingham Plastic Model

The Bingham plastic model describes time-independent fluids. It is a two-parameter rheological model that commonly used in the drilling industry. For the Bingham plastic fluids, initial stress is required to initiate the flow. The modeled shear stresses can be calculated by the following equations.

$$\tau = \mu_p \gamma + \tau_y \dots\dots\dots (3.13)$$

$$\mu_p = \theta_{600} - \theta_{300} \dots\dots\dots (3.14)$$

$$\tau_y = \theta_{300} - \mu_p \dots\dots\dots (3.15)$$

Where: μ_p = Plastic viscosity, cp; τ_y = Yield point, lbs/100ft²

3.3.3.3 Power Law Model

Power law model describe the flow behavior of Pseudoplastic fluid is a two-parameter rheological model. Here the viscosity of power law fluid decreases with increasing shear rate. No initial stress is required for initiating the flow. The Power law relationship is defined as:

$$\tau = k\gamma^n \dots\dots\dots (3.16)$$

Where K is the consistence index, n is the flow behavior index.

$$n = 3.32 \log \left(\frac{\theta_{600}}{\theta_{300}} \right) \dots\dots\dots (3.17)$$

$$K = \frac{510 \times \theta_{300}}{511^n} \text{ dyne sec}^n / 100 \text{ cm}^2 \dots\dots\dots (3.18)$$

3.3.3.4 API Model

A modified Power Law model is recommended in the API RP 13D for the calculation of frictional pressure losses. The advantage of API power law model is it matches the shear rates from viscometer with shear rates inside the drill pipe and annulus. Usually the viscometer readings of θ_{600} and θ_{300} are used for rheology and pressure loss calculations. Inside the annulus, θ_{300} and

θ_{100} are used for rheology and pressure loss calculations. In a Power Law model, increasing shear rate decreases apparent viscosity. The first three shear rates represent the high shear rate in the drill pipe; the next three shear rates represent the low shear rate in the annulus. API model parameters are calculated according to:

$$\tau = k\gamma^n \dots\dots\dots (3.16)$$

$$\text{For Pipe Flow: } n_p = 3.32 \log\left(\frac{\theta_{600}}{\theta_{300}}\right), \quad k_p = \frac{5.11\theta_{600}}{1022^{n_p}} \dots\dots\dots (3.19)$$

$$\text{For Annulus Flow: } n_a = 0.657 \log\left(\frac{\theta_{100}}{\theta_3}\right), \quad k_a = \frac{5.11\theta_{100}}{170.2^{n_a}} \dots\dots\dots (3.20)$$

3.3.3.5 Herschel-Bulkley Model

The Herschel-Bulkley model is Power law model, which accommodates the existence of a yield point. It is a three-parameter rheological model. Herschel-Bulkley model parameters are calculated according to:

$$\tau = \tau_y + k\gamma^n \dots\dots\dots (3.21)$$

$$\tau_y = 2\theta_3 - \theta_6 \dots\dots\dots (3.22)$$

The parameter τ_0 is the actual yield point of drilling fluid, which indicates the lowest shear stress that propels the fluid to flow. It is not an extrapolated value, so it means completely different with the Bingham yield point τ_y . The value of τ_0 is related to the type and concentration of the polymer agents, besides the solid content also affects it. The shear stresses can be calculated by the following equations and shown as follows.

$$n = 3.32 \log\left(\frac{\theta_{600} - \tau_0}{\theta_{300} - \tau_0}\right) \dots\dots\dots (3.23)$$

$$K = \frac{(\theta_{300} - \tau_0)}{511^n} \dots\dots\dots (3.24)$$

3.4 Hydraulics

Hydraulic power is one of the most important hydraulic parameters that have a major impact on the rate of penetration. It is one of the principal functions of drilling fluid is transferring hydraulic power.

3.4.1 Frictional Pressure Loss Calculation

We used the best-fit rheological model of the fluid that has been selected and the rheological properties of fluid have been determined. The next step is to calculate the friction factor, f , which is relevant to the fluid rheological properties and Reynolds number. Once the friction number has been determined, the frictional pressure loss can be calculated using the API Power Law rheological model are as follows:

- Pipe Flow

- a. Pipe velocity:

$$V_p = \frac{0.408q}{D_p^2} \dots\dots\dots(3.25)$$

- b. Reynolds number:

$$N_{Re} = \frac{928D_p V_p \rho}{\mu_e} \dots\dots\dots (3.26)$$

$$\mu_e = 100k \left(\frac{96v_p}{D_p}\right)^{n-1} \left(\frac{3n+1}{4n}\right)^n \dots\dots\dots (3.27)$$

$$n = 3.32 \log \left(\frac{R_{600}}{R_{300}}\right) \dots\dots\dots (3.28)$$

$$k = \frac{5.1R_{600}}{1022^n} \dots\dots\dots (3.29)$$

Where μ_e is the equivalent viscosity, cp

- c. Critical Reynolds number value, $N_{Rec}=2100$

- d. Fanning friction factor:

For laminar flow, $N_{Re} < N_{Rec}$

$$f = 16/N_{Re} \dots\dots\dots (3.30)$$

For turbulent flow, $N_{Re} > N_{Rec}$

$$f = \frac{a}{N_{Re}^b} \dots\dots\dots (3.31)$$

$$a = \frac{\log n + 3.93}{50} \dots\dots\dots (3.32)$$

$$b = \frac{1.75 - \log n}{7} \dots\dots\dots (3.33)$$

e. Frictional pressure loss calculation inside drillstring, ΔP_{ds} :

$$\left(\frac{dp}{dL}\right) = \frac{fv_p^2 \rho}{25.81 D_p} \dots\dots\dots (3.34)$$

$$\Delta P_{ds} = \left(\frac{dp}{dL}\right) \Delta L \dots\dots\dots (3.35)$$

Where (dp/dL) is the pressure gradient, psi/ft.

- Annulus Flow

a. Annular velocity:

$$V_a = \frac{0.408q}{(D_2^2 - D_1^2)} \dots\dots\dots (3.36)$$

b. Reynolds number:

$$N_{Re} = \frac{928(D_2 - D_1)V_a \rho}{\mu_e} \dots\dots\dots (3.37)$$

$$\mu_e = 100k \left(\frac{144v}{D_2 - D_1}\right)^{n-1} \left(\frac{2n+1}{3n}\right)^n \dots\dots\dots (3.38)$$

$$n = 0.657 \log \left(\frac{R_{100}}{R_3}\right) \dots\dots\dots (3.39)$$

$$k = \frac{5.10\theta_{100}}{170.2^n} \dots\dots\dots (3.40)$$

c. Critical Reynolds number value, $N_{Rec} = 2100$

d. Fanning friction factor:

Compare N_{Re} and N_{Rec} to determine the flow regime, use the same procedure as in pipe flow, but the friction factor for laminar flow should be changed as: $f = 24/N_{Re}$.

e. Frictional pressure loss calculation in the annulus, ΔP_a :

$$\left(\frac{dp}{dL}\right) = \frac{fv_a^2\rho}{25.81(D_2-D_1)} \dots\dots\dots (3.41)$$

$$\Delta P_a = \left(\frac{dp}{dL}\right) \Delta L \dots\dots\dots (3.42)$$

- Frictional pressure losses across the bit, ΔP_b :

$$\Delta P_b = \frac{156\rho q^2}{(D_{N1}^2+D_{N2}^2+D_{N3}^2)^2} \dots\dots\dots (3.43)$$

Where D_{N1} , D_{N2} , D_{N3} are diameters of the three nozzles.

- The pump pressure, ΔP_p :

$$\Delta P_p = \Delta P_s + \Delta P_{ds} + \Delta P_b + \Delta P_a \dots\dots\dots (3.44)$$

Where ΔP_s is frictional pressure loss in the surface equipment.

From the above equations, the total pump pressure of an actual drilling operation can be predicted.

CHAPTER 4: RESULTS AND DISCUSSION

In this section, the results of the viscometer test are reported. These data are then analyzed for model selection. A sample hydraulics calculation is calculated, and the results are discussed.

4.1 Fann Viscometer Reading

The rheological parameters of designed drilling fluid systems, a FANN Model 35 Viscometer was used in the experiment. The viscosity of the samples has been measured at the rotational velocity (v) of 3, 6, 100, 200, 300 and 600 rpm. The dial reading (θ) at different rotational velocity are reported in Table 4.1 and Table 4.2. Three trials were conducted for two sample fluids (Fluid-1 & Fluid-2).

Table 4.1: Fann Viscometer Reading: Fluid-1

RPM (v)	Reading ($\bar{\theta}$)	Variance (δ_{θ})
600	39	0.33
300	25	0.58
200	19	0.25
100	11	0.00
6	3	0.08
3	1	0.08

Table 4.2: Fann Viscometer Reading: Fluid-2

RPM (v)	Reading ($\bar{\theta}$)	Variance (δ_{θ})
600	37	0.25
300	23	0.58
200	18	0.08
100	10	0.08
6	2	0.08
3	1	0.00

4.2 Error Analysis

Sample fluids were tested in the temperature of 20°C (Room temperature) using the Fann Viscometer with the speed range of 3-600 rpm (Shear rate of maximum, 1024 s⁻¹). The deflection in degrees of the bob was read from the graduated scale on the dial. The viscosity of the sample was measured at the rotational velocity of 3, 6, 100, 200, 300 and 600 rpm. The set of experimental data or measurements were taken as deflection in degrees of the bob for three times with the speed range of 3-600 rpm for both fluid samples (Fluid-1 & Fluid-2). The average $\bar{\theta}$, and variance δ_{θ} was calculated is reported in Table 4.1 & Table 4.2. $\bar{\theta}$ used in the calculations with the speed range of 3-600 rpm to calculate rheology properties. The standard deviation was found to be in an acceptable range in both cases. In the validation process, we have compared the second set of known fluid data as Fluid-2, and found good comparison results accordingly with the results of Fluid-1.

4.3 Shear stress measured

The shear stresses and shear rates were estimated using equations (4.1 & 4.2) as function of viscosity are shown in Table 4.3 & Table 4.4 for both fluids. The standard deviation was found to be in an acceptable range for both measured shear stresses. The average measured $\bar{\tau}$ of both fluids were used in the calculations and compared with the modeled shear stresses for each rheological model.

$$\gamma = 1.703v \dots\dots\dots (4.1)$$

$$\tau = 1.067\theta \dots\dots\dots (4.2)$$

Table 4.3: Shear stress measured in field units (lb/ft²) for Fluid-1

Shear rate, γ (s ⁻¹)	Shear stress, $\bar{\tau}$ (lbs/100ft ²)	Variance ($\delta\tau$)
1021.80	41.61	0.38
510.90	26.68	0.66
340.60	20.27	0.28
170.30	11.74	0.00
10.22	3.20	0.09
5.11	1.07	0.09

Table 4.4: Shear stress measured in field units (lb/ft²) for Fluid-2

Shear rate, γ (s ⁻¹)	Shear stress, $\bar{\tau}$ (lbs/100ft ²)	Variance ($\delta\tau$)
1021.80	39.48	0.28
510.90	24.54	0.66
340.60	19.21	0.09
170.30	10.67	0.09
10.22	2.13	0.09
5.11	1.07	0.00

4.4 Rheological Model Selection

4.4.1 Newtonian Model and Experiment data

4.4.1.1 Shear stress calculation

Table 4.5 shows the shear stress calculated using the Newtonian model as follows. According to the dial reading of the Fluid-1 solution at 20°C, the data will follow through this model selection process for Newtonian model.

Table 4.5: Comparison analysis between measured and calculated shear stresses

Shear rate (s^{-1})	Measured Shear stress (lbs/100ft ²)	Modeled Shear stress (lbs/100ft ²)
1021.80	41.61	53.35
510.90	26.68	26.68
340.60	20.27	17.78
170.30	11.74	8.89
10.22	3.20	0.53
5.11	1.07	0.27

4.4.1.2 Correlations Analysis

In figure 4.1, residual plot shows the residuals on the vertical axis and the shear stress on the horizontal axis. The plot pattern is U-shaped, which suggests that a better fit as a non-linear model.

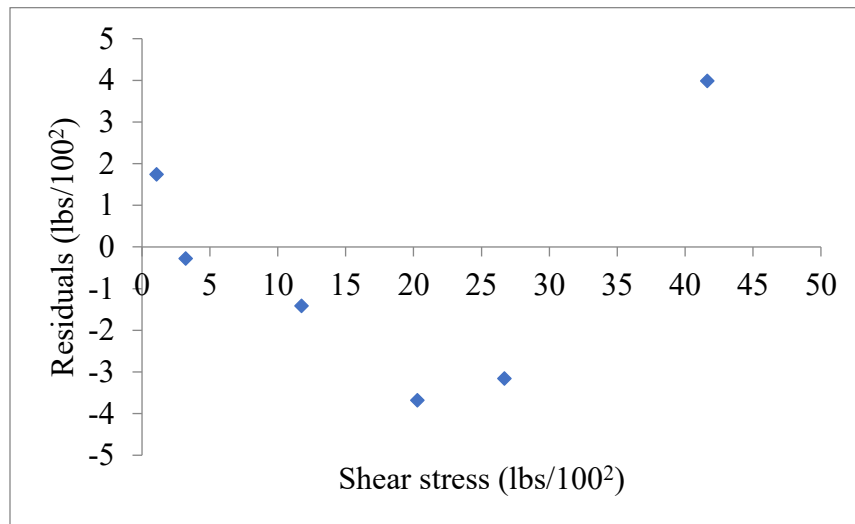


Figure 4.1: Residual plot for measured and calculated shear stress for Newtonian model.

Therefore, on the basis of this residual plot analysis, we plotted the shear rate versus shear stress of measured and calculated data for Newtonian model. Then comparing both with respect to shear rate in the x-axis, we compared the trend for measured and calculated shear stress (Figure

4.2). We checked the linear relationship between measured and modeled shear stresses. From this relationship comparison analysis, we found a regression value of $R^2 = 0.9713$ (Table-4.10).

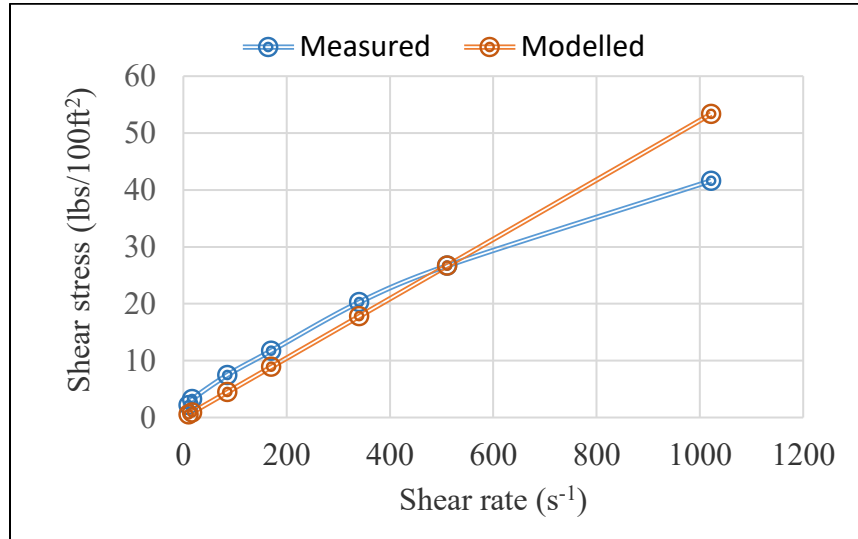


Figure 4.2: Plot for shear rate vs. shear stress of measured and modeled data using Newtonian model.

4.4.1.3 The absolute average percent of error (E_{AAP}) analysis

From this statistical method, we used to calculate the E_{AAP} , the model that provide the lowest E_{AAP} is selected to be the best one.

$$E_{AAP} = \left[\left(\frac{1}{N} \right) \sum |(\tau_{measured} - \tau_{calculated}) / \tau_{measured}| \right] \times 100 \dots \dots \dots (4.3)$$

A comparison of measured and calculated data in the above Figure 4.2. By using the above E_{AAP} equation (4.3) for the Newtonian model, $E_{AAP} = 31.87\%$.

4.4.2 Bingham Plastic Model and Experiment data

4.4.2.1 Shear stress calculation

Table 4.6 described the result of calculated shear stress using the Bingham Plastic model as follows. According to the dial reading of the fluid sample at 20°C, the data will follow through this model selection process for Bingham Plastic model.

Table 4.6: Comparison analysis between measured and calculated shear stresses

Shear rate (s-1)	Measured Shear stress (lbs/100ft ²)	Modeled Shear stress (lbs/100ft ²)
1021.80	41.61	41.23
510.90	26.68	25.70
340.60	20.27	19.84
170.30	11.74	14.11
10.22	3.20	8.19
5.11	1.07	5.87

4.4.2.2 Correlations Analysis

In Figure 4.5, residual plot for measured shear stress and calculated shear stress showed that the plot pattern is not random and is U-shaped, which suggest that a better fit for a non-linear model. So, the calculated shear stress has the exponential trend line better than linear trend line and has highest regression value that give best correlation measurement for Bingham Plastic model.

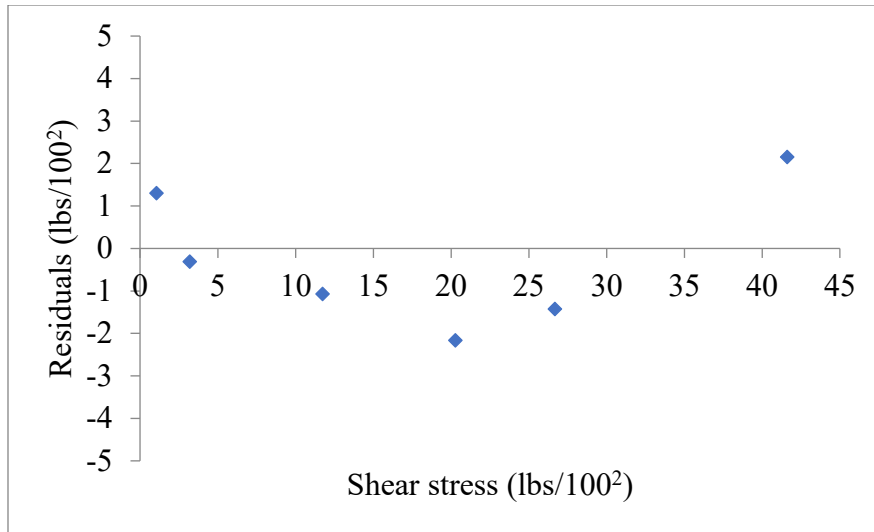


Figure 4.3: Residual plot for measured and calculated shear stress for Bingham Plastic model

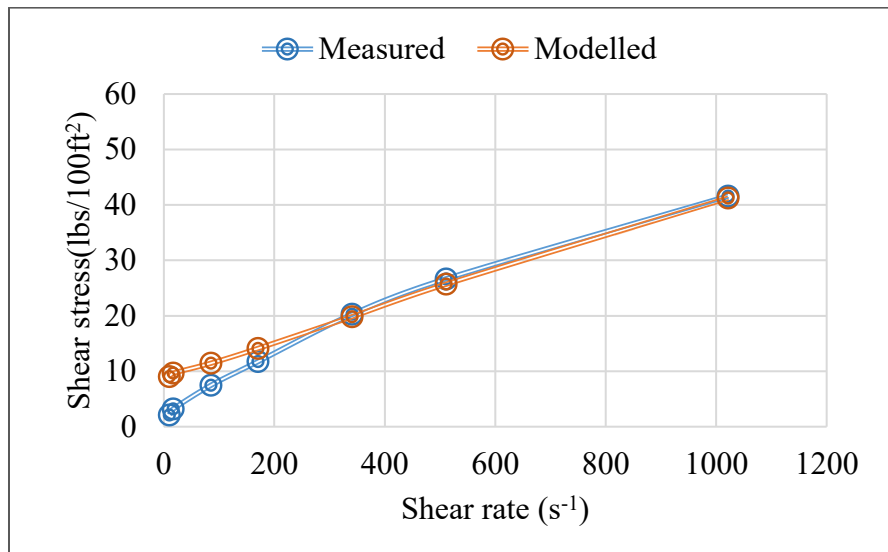


Figure 4.4: Plot for shear rate vs. shear stress of measured and Modeled data

Therefore, based on this residual plot analysis, we plotted measured and calculated shear stress with shear rate, then comparing the analysis, we found best correlation regression value in exponential power regression line for measured and calculated shear stress. We also checked the linear relationship between measured and modeled shear stresses. From this relationship of comparison analysis, we found a regression value of $R^2 = 0.9898$ (Table-4.10).

4.4.2.3 The absolute average percent of error (EAAP) analysis

The Bingham plastic model E_{AAP} is **90.42%**. Above figure shows a comparison between measured and calculated data, which is worse than the Newtonian model.

4.4.3 Power Law Model and Experiment data

4.4.3.1 Shear stress calculation

Table 4.7: The measured and calculated shear stresses

Shear rate (s^{-1})	Measured Shear stress (lbs/100ft ²)	Modeled Shear stress (lbs/100ft ²)
1021.80	41.61	41.32
510.90	26.68	26.52
340.60	20.27	20.46
170.30	11.74	13.13
10.22	3.20	2.17
5.11	1.07	1.39

4.4.3.2 Correlations Analysis

In Figure 4.5, residual plot for measured shear stress and calculated shear stress showed that the plot pattern is random, which suggest a better fit for a linear model. The calculated shear stress fits within a linear trend line.

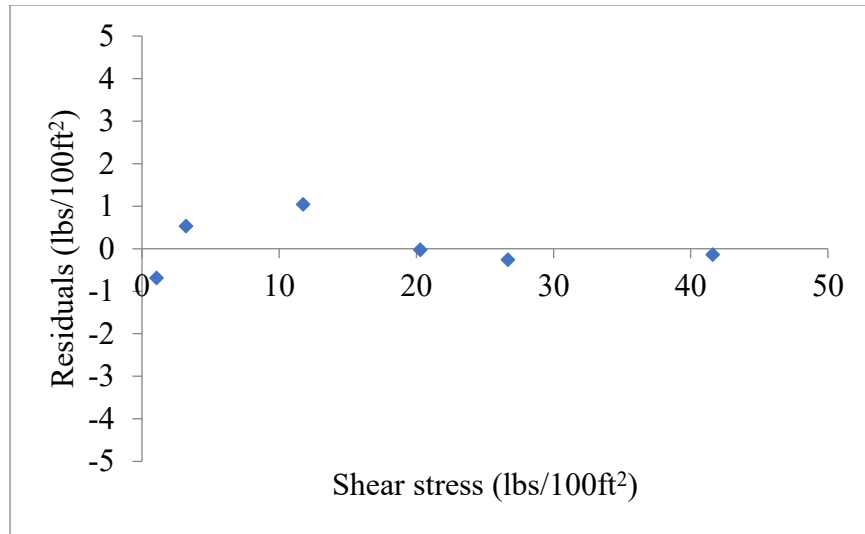


Figure 4.5: Residual plot for measured and calculated shear stress for Power Law model.

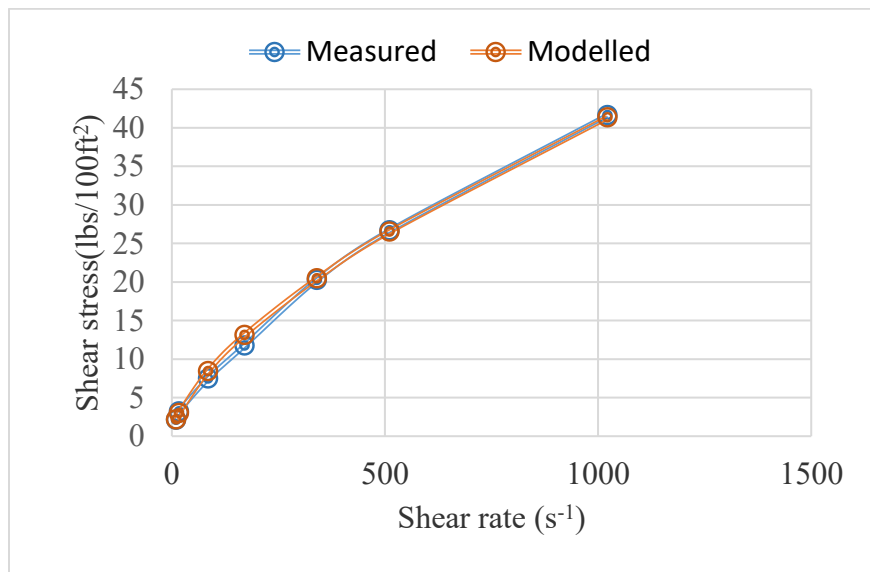


Figure 4.6: Plot for shear rate vs. shear stress of measured and calculated data

Therefore, on the basis of this residual plot analysis, the two lines between measured and calculated shear stress with shear rate for Power Law model. Then comparing result found best correlation regression value in linear regression line for measured and calculated shear stresses

(Figure 4.6). Therefore, on the basis of this linear correlation comparison analysis, we found highest regression value of $R^2 = 0.9992$ (Table-4.10).

4.4.3.3 The absolute average percent of error (EAAP) analysis

The Power Law model E_{AAP} is 10.96%. Figure 4.6 shows a comparison between measured and calculated data, which gives the better result than the Newtonian and Bingham Plastic Model.

4.4.4 API Model and Experiment data

4.4.4.1 Shear stress calculation

Table 4.8 The measured and calculated shear stresses

Shear rate (s-1)	Measured Shear stress (lbs/100ft ²)	Modeled Shear stress (lbs/100ft ²)
1021.80	41.61	41.91
510.90	26.68	27.20
340.60	20.27	19.66
170.30	11.74	11.69
10.22	3.20	2.23
5.11	1.07	1.02

4.4.4.2 Correlations Analysis

Figure 4.8 shows the residual plot for measured shear stress and calculated shear stress. The plot pattern is random, which suggest a better fit for a linear model.

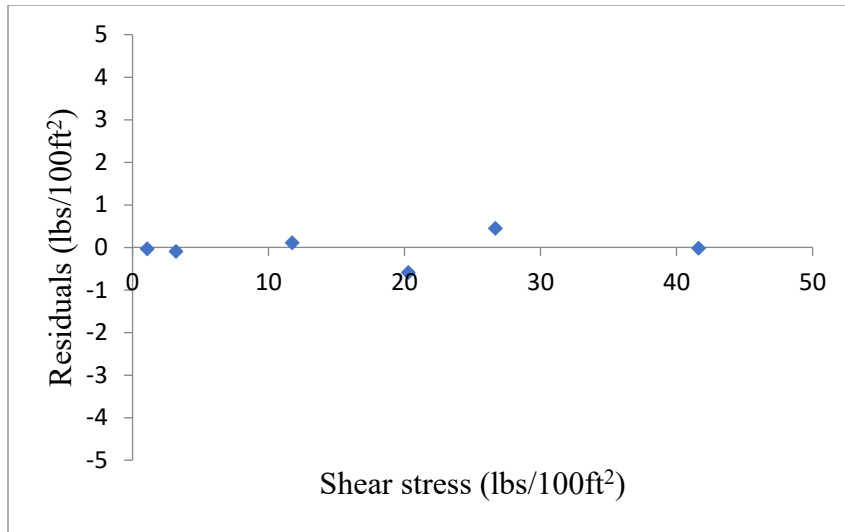


Figure 4.7: Residual plot for measured and calculated shear stress for API model.

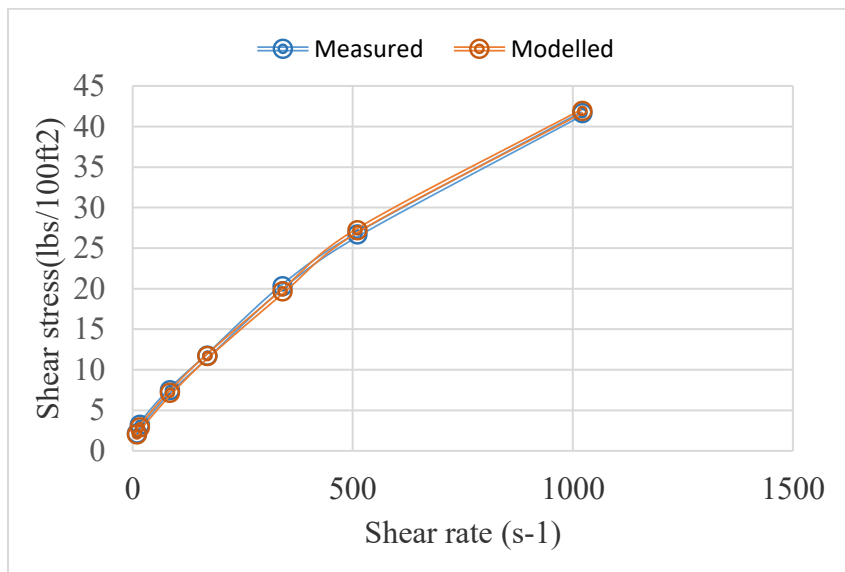


Figure: 4.8: Plot for shear rate vs. shear stress of measured and calculated data.

Therefore, on the basis of this residual plot analysis, we plotted two lines in Figure 4.8 between measured and calculated shear stress with shear rate for API Power Law model. Therefore, on the basis of these linear correlation comparison analysis, we found a regression value of $R^2 = 0.9992$ (Table-4.10).

4.4.4.3 The absolute average percent of error (EAAP) analysis

The API model E_{AAP} is 5.84%, which is better result than the previous three models.

4.4.5 Herschel-Bulkley Model and Experiment data

4.4.5.1 Shear stress calculation

Table 4.9 The measured and calculated shear stresses

Shear rate (s^{-1})	Measured Shear stress (lbs/100ft ²)	Modeled Shear stress (lbs/100ft ²)
1021.80	41.61	39.77
510.90	26.68	24.83
340.60	20.27	18.60
170.30	11.74	11.89
10.22	3.20	2.89
5.11	1.07	1.76

4.4.5.2 Correlations Analysis

In Figure 4.9, residual plot for measured shear stress and calculated shear stress showed that the plot pattern is random, which suggest a better fit for a linear model

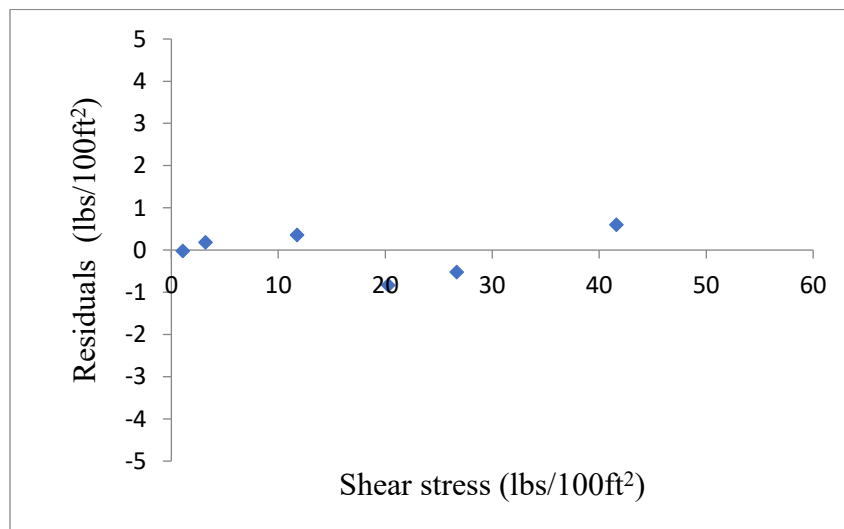


Figure 4.9: Residual plot for measured and calculated shear stress for Herschel-Bulkley.

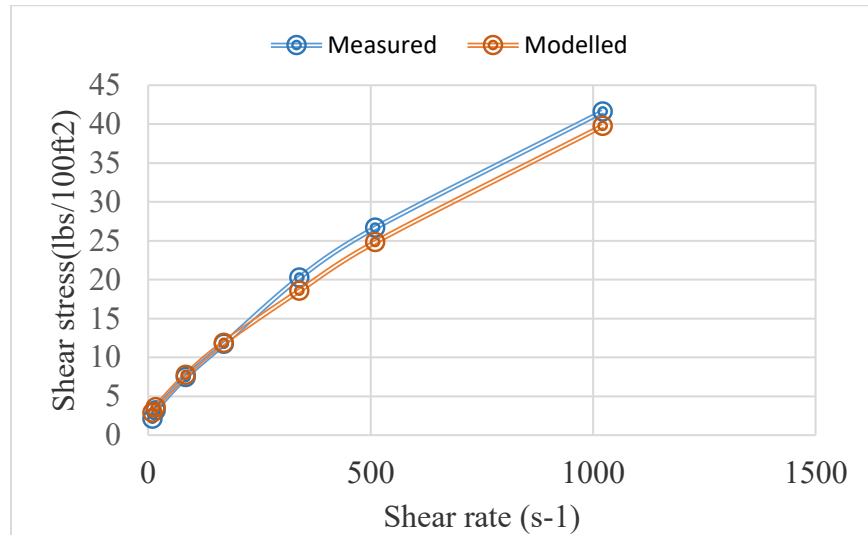


Figure 4.10: Plot for shear rate vs. shear stress of measured and calculated data for Herschel-Bulkley model.

Therefore, on the basis of this residual plot analysis, we plotted two regression lines between measured and calculated shear stress for Herschel-Bulkley model in Figure 4.10. On the basis of this linear correlation comparison analysis, we found the regression value is $R^2 = 0.9984$.

4.4.5.3 The absolute average percent of error (EAAP) analysis

In the Herschel-Bulkley Model, we found E_{AAP} is 13.65%, (Figure 4.12). which gives better results than the first three models but compares favorably to the API model.

4.5 Summary of rheological model selection

According to Table 4.10, the API Power Law model provides the lowest E_{AAP} and highest R^2 value for Fluid-1.

Table 4.10: Summary of best regression equation for non- linear and linear models for each rheological model selection for Fluid-1

Model Name	Regression equation	R^2	E_{AAP}
Newtonian	$y = 1.2913x - 4.5877$	0.9713	31.87%
Bingham	$y = 0.8454x + 4.4232$	0.9898	90.42%
Power Law	$y = 0.9945x + 0.1655$	0.9973	10.96%
API Power Law	$y = 1.0213x - 0.5137$	0.9992	5.84%
Hershel-Bulkley	$y = 0.9372x + 0.2903$	0.9984	13.65%

The API Power Law Model can better describe the flow behavior of fluids solution in comparing with other rheological models. Therefore, we can strongly conclude that most of the polymer/mud solutions are Pseudoplastic fluid. Here the API Power Law Model accurately represents the rheological properties of drilling fluid in drill pipe and annulus. We have used this API power law model precisely to estimate the frictional pressure loss and calculate the bit hydraulics.

It was also found that the best rheological model was fitted with API Power-law model has the lowest E_{AAP} of 6.64% (Table 4.11) for Fluid-2. Therefore, in the validation process, we have compared this set of known fluid data as Fluid-2, and found good comparison results accordingly with the results of Fluid-1.

Table 4. 11: Summary of best regression equation for non- linear and linear models for each rheological model selection for Fluid-2

Model Name	Regression equation	R ²	E _{AAP}
Newtonian	$y = 1.2472x - 3.7235$	0.9746	21.40%
Bingham	$y = 0.7582x + 6.7651$	0.9743	70.22%
Power Law	$y = 0.9978x - 0.0324$	0.9988	18.86%
API Power Law	$y = 1.0061x - 0.2489$	0.9997	6.64%
Hershel-Bulkley	$y = 0.9368x - 0.0307$	0.9988	24.30%

4.6 Hydraulics Simulation

A hydraulics simulation was conducted with the data from a well in 420ft of water in Block 89, south pass, Gulf of Mexico (Hareland et al. 2012). The 5-in drilling pipe run to 12349 ft measured depth. The intermediate casing of 11 7/8-in was run to 12710 ft depth. The mud was 11.5 ppg. To simplify the hydraulics simulation, the temperature was assumed to be constant all over the well bore and it is approximate to 68°F (20°C). The rheological data was taken from the test of a fluid polymer system given below (Engineering data). The specific well architecture data was shown. The calculation procedure was listed as follows.

Engineering data from the well design:

Drillpipe-5in. 19.5 S-135 w/4.5 IF (6.75in. ×3in. connection): D1=5in, Dp =4.5in

Casing 117/8 in. × 10.711in., D2=10.711in.

Length of well = 12440ft

Rheological data = same as in table 6.1

Q = 100 GPM

Density (ρ) = 11.55lb/gal

Bit: 10 5/8 in. w/3: 28/32 in. jets

$$\Delta P_s = 0$$

- Pipe Flow

a. Pipe velocity:

$$V_p = \frac{0.408q}{D_p^2} = \frac{0.408 \times 100}{(4.5)^2} = 2.015 \text{ ft/sec}$$

b. Reynolds number:

$$n = 3.32 \log \left(\frac{R_{600}}{R_{300}} \right) = 3.32 \log \left(\frac{37}{23} \right) = 0.685$$

$$k = \frac{5.1R_{600}}{1022^n} = \frac{5.1 \times 37}{1022^{0.685}} = 1.632 \text{ dyne. sec}^n/\text{ft}$$

$$\mu_e = 100k \left(\frac{96v_p}{D_p} \right)^{n-1} \left(\frac{3n+1}{4n} \right)^n$$

$$= 100 \times 1.632 \times \left(\frac{96 \times 2.015}{4.5} \right)^{0.685-1} \left(\frac{3 \times 0.685 + 1}{4 \times 0.685} \right)^{0.685} = 53.884 \text{ cp}$$

$$N_{Re} = \frac{928D_p V_p \rho}{\mu_e} = \frac{928 \times 4.5 \times 2.015 \times 11.55}{53.884} = 1803.513$$

c. Critical Reynolds number value, $N_{Rec} = 2100$

d. Fanning friction factor:

For laminar flow, $N_{Re} < N_{Rec}$

$$f = 16 / Re = 16 / 1803.513 = 0.008872$$

e. Frictional pressure loss calculation inside drillstring, ΔP_{ds} :

$$\left(\frac{dp}{dL} \right) = \frac{f v_p^2 \rho}{25.81 D_p} = \frac{0.008872 \times 2.015^2 \times 11.55}{25.81 \times 4.5} = 0.003581 \text{ psi/ft}$$

$$\Delta P_{ds} = \left(\frac{dp}{dL} \right) \Delta L = 0.003581 \times 12440 = 44.553 \text{ psi}$$

Where (dp/dL) is the pressure gradient, psi/ft.

- Annulus Flow

a. Annular velocity:

$$V_a = \frac{0.408q}{(D_2^2 - D_1^2)} = \frac{0.408 \times 100}{(10.711^2 - 5^2)} = 0.455 \text{ ft/sec}$$

b. Reynolds number:

$$n = 0.657 \log\left(\frac{R_{100}}{R_3}\right) = 0.657 \log\left(\frac{10}{1}\right) = 3.32$$

$$k = \frac{5.10\theta_{100}}{170.2^n} = \frac{5.1 \times 10}{170.2^{3.32}} = 1.508 \text{ dyne. sec}^n/\text{ft}$$

$$\mu_e = 100k\left(\frac{144v}{D_2 - D_1}\right)^{n-1} \left(\frac{2n+1}{3n}\right)^n = 100 \times 1.508 \left(\frac{144 \times 0.455}{10.711 - 5}\right)^{3.32-1} \left(\frac{2 \times 3.32 + 1}{3 \times 3.32}\right)^{3.32} = 29.022$$

$$N_{Re} = \frac{928(D_2 - D_1)V_a \rho}{\mu_e} = \frac{928 \times (10.711 - 5) \times 0.455 \times 11.55}{29.022} = 959.095$$

c. Critical Reynolds number value, $N_{Rec} = 2100$

d. Fanning friction factor:

For laminar flow, $N_{Re} < N_{Rec}$

$$f = 24 / Re = 16 / 959.095 = 0.025$$

e. Frictional pressure loss calculation inside annulus, ΔP_a :

$$\left(\frac{dp}{dL}\right) = \frac{f v_p^2 \rho}{25.81(D_2 - D_1)} = \frac{0.025 \times 2.015^2 \times 11.55}{25.81 \times (10.711 - 5)} = 0.000405 \text{ psi/ft}$$

$$\Delta P_a = \left(\frac{dp}{dL}\right) \Delta L = 0.003581 \times 12440 = 5.043 \text{ psi}$$

- Frictional pressure losses across the bit, ΔP_b :

$$\Delta P_b = \frac{156\rho q^2}{(D_{N1}^2 + D_{N2}^2 + D_{N3}^2)^2} = \frac{156 \times 11.2 \times 100^2}{(28^2 + 28^2 + 28^2)^2} = 3.257 \text{ psi}$$

- The pump pressure, ΔP_p :

$$\Delta P_p = \Delta P_s + \Delta P_{ds} + \Delta P_b + \Delta P_a = 0 + 44.553 + 3.257 + 5.043 = 52.853 \text{ psi}$$

From the above simulation, the pump pressure of an actual drilling operation was predicted. The estimated pump pressure refers to the power lost overcoming the friction through the drilling fluid circulation, which is an important parameter in drilling engineering design.

4.7 Data used to validate the approach

Accurate downhole and surface measurements of a synthetic-based drilling fluid were taken in a well to determine variances between actual and calculated pump pressure. A special team headed by Marathon Oil Co. successfully instrumented and collected a very large volume of hydraulics data on a well in the Gulf on Mexico at 12,710 ft depth. Using multiple sensor packages, accurate measurement of downhole dynamic pressure (hydraulic data) were obtained. The well selected for the test was in 420 ft of water in Block 89, South Pass, Gulf of Mexico. Testing was conducted after running and cementing a single-weight intermediate string of 11 7/8-in. casing to 12,710 ft. The mud was the same 11.5 lbm/gal polyaphaolefin (PAO)-based drilling fluid used to drill the long, intermediate casing interval. A single mud pit was isolated to limit surface volume to about 220 bbl and to minimize circulating time for conditioning mud. This also reduces temperature variations while the mud was on the surface. The temperature seems to be constant during the test and it is approximate to 150°F. In addition to conventional rheological measurements, HPHT properties were taken using a Fann Model 35 viscometer.

Table 4.12: Average % of reduction error difference between field and modeled SPP

DEPTH [m]	SPP_FLD [kPa]	SPP_API Model [kPa]	%ERROR	Avg. % Error
600	10656	8924	16	14
620	11230	9188	18	
640	11291	8998	20	
660	9877	8809	11	
680	10852	9074	16	
700	10332	8883	14	
720	10341	9035	13	
740	10133	8957	12	
760	10109	8995	11	
780	9937	8917	10	
800	9848	8928	9	

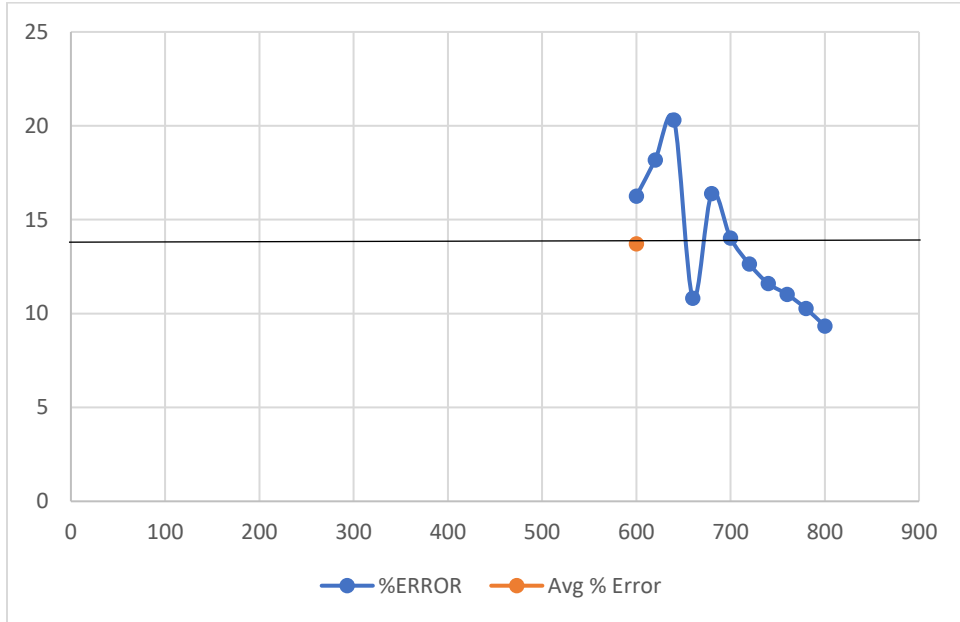


Figure 4.11: Average % of reduction error difference between field SPP and modeled SPP

According to the above testing facilities the field drilling data and modelled drilling data were compared (using API model) in terms of SPP (Total pressure loss/Stand pipe pressure) showed in the above Table 4.12. This results also described in the figure 4.11. It is clearly shown that the difference between SPP-field and SPP-API modeled average error was 14%, which is the acceptable average percentage of error range in the drilling industry. Therefore, API hydraulics calculation give a good approximation to measured total pump pressure with 14% of difference between measured and calculated data.

CHAPTER 5: CONCLUSIONS AND FUTURE WORK

5.1 Summary

- The drilling fluid rheological properties were obtained from the laboratory experiments to analyse/design drilling fluid system.
- The rheological models, Newtonian, Bingham, Power-law, API RP 13D, Herschel-Bulkley, have been evaluated for accurate representation. Among these models, API models gave comparatively better result.
- A simple and direct approach has been presented for selecting the best rheological model for any drilling fluid system according to the lowest E_{AAP} error analysis criteria.
- The API model can be applied with high confidence to predict rheological properties and hydraulics calculations in water based or oil-based mud. Also, this model can fit adequately many real yield stress fluids, with simply two parameters.
- The proposed methods by predicting pressure losses can be applied to correcting frictional coefficient/ bit wear/ fluid loss effects. The results were more accurate than those obtained with standards method using other models.
- The study concluded the hydraulic effects and to increase drilling efficiency via mud conditioning and hydraulics optimization.

5.2 Further considerations

Considering the approaches of this study and model calculations/recommendations is important as it gives us a major range to evaluate the rheological models as well as well log in corrections. Also, it gives as a result, a better interpretation and validation the study proposed for the future research.

In this study, the pump pressure of an actual drilling operation was collected from filed data. The estimated total pump pressure refers to the power loss calculations, overcoming the friction through the drilling fluid operation is an important parameter in drilling engineering design. The hydraulic engineering calculations done the individual and total frictional pressure losses in the well fluid circulating system with the rheological models. These pressure losses of SPP can be compared to the field SPP to estimate the maximum performances of drilling operations. The models help to prevent major problems in drilling circulations such as stuck pipe, reducing bit wear, high cost of well-login operations by applying this study of approaches to determining the optimum flow needed to improve drilling operation.

References

Abdo, J., and Haneef, D. "Nanoparticles: Promising solution to overcome stern drilling problems". NSTI-Nanotech 2010, www.nsti.org, ISBN 978-1-4398-3415-2, Vol. 3.

Amanullah, M. SPE, Al-Arfaj, M. K, and Al-Abdullatif, Z. "Preliminary Test Results of Nano-based Drilling Fluids for Oil and Gas Field Application". SPE/IADC Drilling Conference and Exhibition held in Amsterdam, The Netherlands, 1–3 March 2011.

Amanullah, MD., and Al-Abdullahtif, Z. "Preliminary test results of a water based nanofluid". The 8th International Conference & Exhibition on Chemistry in Industry, Manama, Bahrain, 18-20, October 2010.

American Petroleum Institute. "Recommended Practice on the Rheology and Hydraulics of Oil-Well Drilling Fluids". API RP 13D, 3rd Edition, Washington, DC, June 1995.

Awele, N. 2014. "Investigation of Additives on Drilling Mud Performance With 'TONDER GEOTHERMAL DRILLING' As A Case Study", Master Thesis, Aalborg University Esbjerg, Denmark.

Cranford, P.J., Gordon, Jr., D.C., Lee, K., Armsworthy, S.L., Tremblay, G.-H. 1999. Chronic toxicity and physical disturbance effects of water- and oil-based drilling fluids and some major constituents on adult sea scallops (*Placopecten magellanicus*). *Marine Environmental Research*, Vol. 48, Issue 3, pp. 177-262.

Darley, H. C. H. and Gary, G. R. 1988. *Composition and Properties of Drilling and Completion Fluids*. Gulf Publishing Company, Houston, TX, 5th Ed, 1988.

Davison, J.M., Clary, S., Saasen, A., Allouche, M., Bodin, D. 1999. "Rheology of Various Drilling Fluid Systems Under Deepwater Drilling Conditions and the Importance of Accurate Predictions of Downhole Fluid Hydraulics," paper SPE 56632 presented at the 1999 SPE Annual Technical Conference, Houston, 3-6 October.

De Wolfe, R. C., Coffin, G. B. and Byrd, R. V. "Effects of Temperature and Pressure on Rheology of Less Toxic Oil Muds". SPE 11892 presented at Offshore Europe, Aberdeen, UK, 6-9 September 1983.

Demirdal, B., and Cunha, J.C. "Importance of Drilling Fluids 'Rheological and Volumetric Characterization to Plan and Optimize Managed Pressure Drilling Operations". *Journal of Canadian Petroleum Technology*. February 2009, Volume 48, No. 2.

El-Diasty, A. I., Ragab, A. M. S. “Applications of Nanotechnology in the Oil & Gas industry: Latest Trends Worldwide & Future Challenges in Egypt”. North Africa Technical Conference & Exhibition held in Cairo, Egypt, 15–17 April 2013

Friedheim, J., Young, S., Stefano, G. D., Lee, J., and Guo, Q. “Nanotechnology for Oilfield Applications-Hype or Reality”. SPE International Oilfield Nanotechnology Conference held in Noordwijk, The Netherlands, 12-14 June 2012.

Garvin, T. R. and Moore, P. L. “A Rheometer for Evaluating Drilling Fluids at Elevated Temperatures”. SPE 3062 presented at the Fall Meeting of the Society of Petroleum Engineers of AIME, Houston, TX, 4-7 October 1970.

Growcock, F.B. and Frederick, T.P., Operational Limits of Synthetic Drilling Fluids; SPE Drilling & Completion, Vol. 11, No. 3, pp. 132-136, September 1996.

Growcock, F.B., Andrews, S.L. and Frederick, T.P., Physicochemical Properties of Synthetic Drilling Fluids; paper SPE 27450 presented at the SPE/IADC Drilling Conference, Dallas, TX, 15-18 February 1994.

Gusler, W., M. Pless, J. Maxey, P. Grover, J. Perez, J. Moon and T. Baaz. 2007. A new extreme hph viscometer for new drilling fluid challenge. SPE Drilling and Completion, 81, June 2007.

Hemphill, T., Prediction of Rheological Behavior of Ester-Based Drilling Fluids Under Downhole Conditions; paper SPE 35330 presented at the International Petroleum Conference and Exhibition of Mexico, Villahermosa, Mexico, 5-7 March 1996.

Herzhaft, B., Ragouillaux, A., and Coussot, P. 2006. How to unify low-shear-rate rheology and gel properties of drilling muds: a transient rheological and structural model for complex well applications. The IADC/SPE Drilling Conference held in Miami, Florida, U.S.A., 21–23 February.

Herzhaft, B., Rousseau, L., Neau, L., Moan, M. and Bossard, F. 2002. “Influence of Temperature and Clays/Emulsion Microstructure on Oil-Based Mud Low Shear Rate Rheology,” paper SPE 86197 presented at the 2002 SPE Annual Technical Conference and Exhibition, San Antonio, 29 September-2 October.

Hoelscher, K.P., Young, S., Friedheim, J., and Stefano, G. D. “Nanotechnology Application in Drilling Fluids”. 11th Offshore Mediterranean Conference and Exhibition in Ravenna, Italy, March 20-22, 2013.

Khodja, M., Canselier, Jean-Paul, Bergaya, Faiza, Fourar, Karim, Malika and Cohaut, Nathalie, Benmounah, and Abdelbaki. 2010a. Shale problems and waterbased drilling fluid optimisation in the Hassi Messaoud Algerian oil field. *Applied Clay Science*, vol. 49 (n° 4). pp. 383-393.

Khodja, M., Khodja-Saber, M., Canselier, J. P., Cohaut, N., and Bergaya, F. 2010b. *Drilling Fluid Technology: Performances and Environmental Considerations. Products and Services; from R&D to Final Solutions*, Igor Fuerstner (Ed.), ISBN: 978-953-307-211-1.

Lee, J., Shadravan, A., and Young, S. 2012. Rheological Properties of Invert Emulsion Drilling Fluid under Extreme HPHT Conditions. IADC/ SPE Drilling Conference and Exhibition held in San Diego, California, USA, 6-8 March 2012.

Maghrabi, S., Wagle, V., Teke, K., Kulkarni, D., and Kulkarni, K. 2011. Low Plastic Viscosity Invert Emulsion Fluid System for HPHT Wells. AADE National Technical Conference and Exhibition held at the Hilton Houston North Hotel, Houston, Texas, held on April 12-14.

Merlo, A., Maglione, R., and Piatti, C. 1995. "An Innovative Model for Drilling Fluid Hydraulics," paper SPE 29259 presented at 1995 SPE Oil and Gas Conference, Kuala Lumpur, 20-22 March.

M-I SWACO. 2009. "M-I SWACO joins Rice University in Nanotech Research Program." Press Release, 28 October.

Minton, R. C. and Bern, P. A. "Field Measurement and Analysis of Circulating System Pressure Drops with Low-Toxicity Oil-Based Drilling Fluids. SPE 17242 presented at the SPE/IADC Drilling Conference, Dallas, TX, 28 February-2 March 1988.

Mohammed, M. A. R., and Mohammed, S. A. A. 2009. Effect of Additives on Rheological Properties of Invert Emulsions. *Iraqi Journal of Chemical and Petroleum Engineering*, Vol.10 No.3, 31-39, ISSN: 1997-4884.

Nwaoji, C. O., Hareland, G., Hussein, M., Nygaard, R., and Zakaria, M. F. "Wellbore Strengthening Nan—Particle Drilling Fluid Experimental Design Using Hydraulic Fracture Apparatus". SPE/ IADC Drilling Conference and Exhibition held in Amsterdam, The Netherlands, 5-7 March 2013.

Politte, M.D. 1985. "Invert Oil Mud Rheology as a Function of Temperature," paper SPE 13458 presented at the 1985 SPE/IADC, New Orleans, 6-8 March.

Power, D. and Zamora, M. 2003. "Drilling Fluid Yield Stress: Measurement Techniques for Improved Understanding of Critical Drilling Fluid Parameters," paper AADE-03-NTCE-35 presented at the 2003 AADE Technical Conference, Houston, 1-3 April.

Proehl, T. and Sabins, F. 2006. Drilling and Completion Gaps for HPHT Wells in Deep Water-Final Report, Department of Interior.

Srivista, T. J. "An Experimental Investigation on use of nanoparticles as Fluid loss Additives in a Surfactant-Polymer Based Drilling Fluid. Texas Tech University, M. Sc. Thesis.

Sushant, A., Phuoc T., Yee S., Donald M., and Rakesh K. G. 2011. Flow Behavior of Nanoparticle Stabilized Drilling Fluids and Effect of High Temperature Aging. AADE-11-NTCE-3.

Taugbol, K., G. Fimreite, O. I. Prebensen, M. I. Sweco, K. Svanes, T. H. Omland, P. E. Svela and D. H. Breivik. 2005. Development and Field Testing of a Unique High Temperature/High Pressure Oil-Based Drilling Fluid with Minimum Rheology and Maximum Sag Stability. Journal of Offshore Technology, 13, 46.

Tehrani, A. 2007. Behaviour of Suspensions and Emulsions in Drilling Fluids. Annual transactions of the nordic rheology society, vol. 15.

Thivolle, S, 2004. "A New Practical Rheology Model for HPHT Fluid," paper presented for M. Eng. degree Texas A&M University. College Station, Texas.

Zakaria, M. F., Husein, M., and Hareland, G. "Novel Nanoparticle-Based Drilling Fluid with Improved Characteristics". SPE International Oilfield Nanotechnology Conference held in Noordwijk, The Netherlands, 12-14 June 2012.

Zamora, M. and Power, D, 2002. "Making a Case for AADE Hydraulics and the Unified Rheological Model," paper AADE-02-DFWM-HO-13 presented at the 2002 AADE Technical Conference, Houston, 2-3 April.